Non-destructive Sensing of Plant-borne Chemicals: Biomarkers, Agrochemicals, and Pollutants

Yi Jing Wong,[a,b] Yifei Luo,*[b] Xian Jun Loh[b] and Xiaodong Chen*[a]

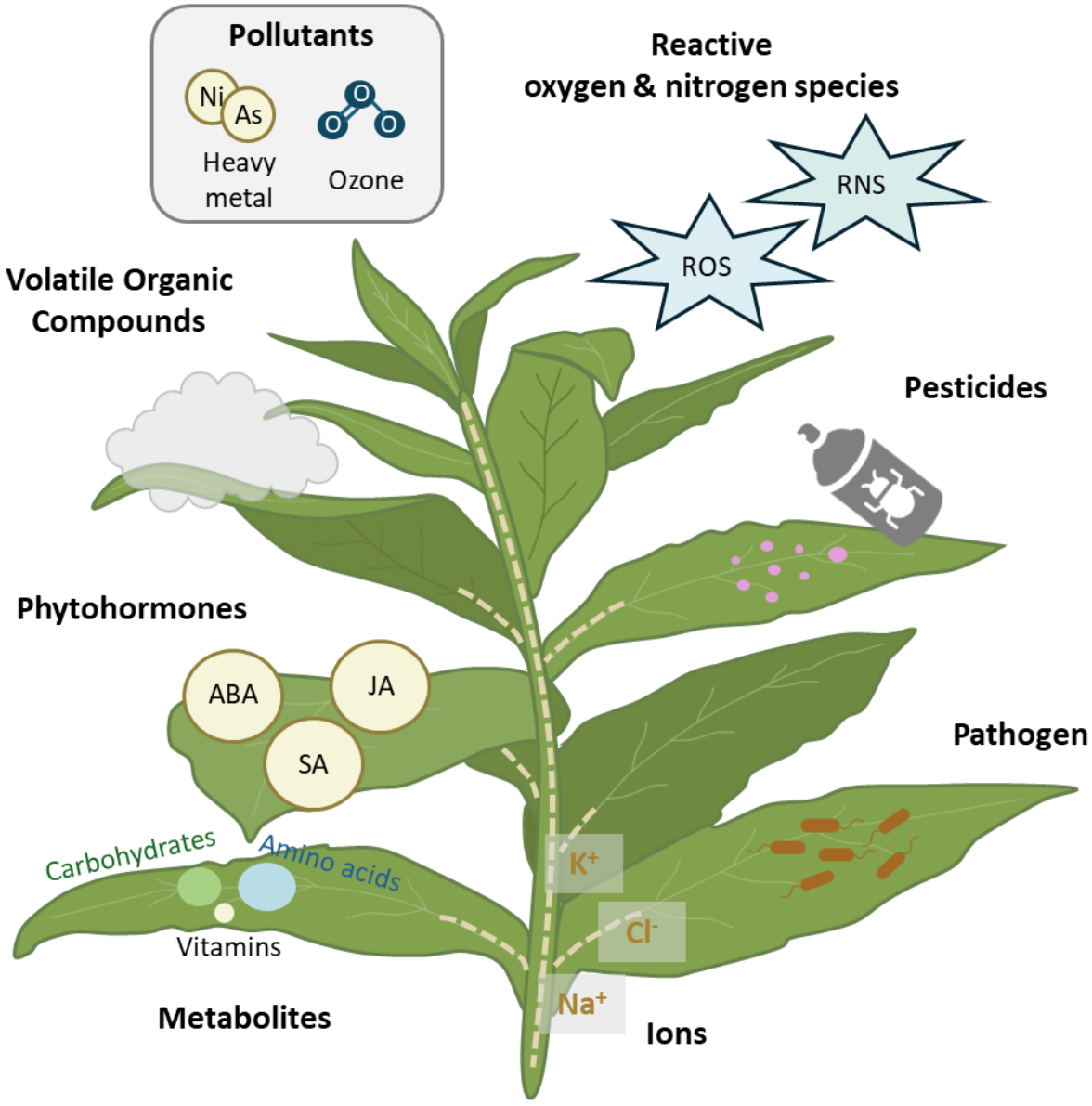

[a] *Innovative Center for Flexible Devices (iFLEX), Max Planck-NTU Joint Lab for Artificial Senses, School of Materials Science and Engineering, Nanyang Technological University, 50 Nanyang Avenue, Singapore 639798, Republic of Singapore*

[b] *Institute of Materials Research and Engineering (IMRE), Agency for Science, Technology and Research (A*STAR), 2 Fusionopolis Way, Innovis #08-03, Singapore 138634, Republic of Singapore*

Correspondence:

*Yifei Luo, Institute of Materials Research and Engineering (IMRE), Agency for Science, Technology and Research (A*STAR), 2 Fusionopolis Way, Innovis #08-03, Singapore 138634, Republic of Singapore. E-mail:* luo_yifei@imre.a-star.edu.sg

Xiaodong Chen, Innovative Center for Flexible Devices (iFLEX), Max Planck-NTU Joint Lab for Artificial Senses, School of Materials Science and Engineering, Nanyang Technological University, 50 Nanyang Avenue, Singapore 639798, Republic of Singapore. Email: chenxd@ntu.edu.sg

Abstract: With the increasing risk of global agricultural instability and the pressing need to enhance crop productivity, monitoring of plant health has become increasingly important. Chemical sensing of agricultural environmental factors and plant signaling molecules has been shown to provide valuable insights into plant growth and development. Recent advances in plant monitoring technologies have seen a shift toward non-destructive, portable or wearable sensors, which offer advantages over traditional analytical instruments, such as faster detection with real-time monitoring capabilities. However, these emerging forms of chemical sensors have not been widely adopted. This review summarizes recent advancements in plant chemical sensing, highlighting key environmental chemicals and plant biomarkers for detection, sensing materials, and detection mechanisms. Finally, the challenges and outlook of chemical sensors for plant monitoring are discussed. Through the identification of the key challenges, we hope to advance the development of non-destructive chemical sensors and facilitate their deployment for in-field plant monitoring.

1. Introduction

The growing risk of global agriculture instability [1-3] has created a pressing need for crop productivity enhancement. [4-6] Significant attention has been focused on the monitoring of plant health during the development process for productivity improvement. Throughout the growth cycle, plants are often exposed to abiotic stresses such as light, temperature, water and biotic stresses from pathogens. These stress factors greatly impact the final crop yield and quality, posing challenges to the agricultural sector. [7] Early recognition of stress conditions for optimization and intervention has therefore become a key priority for plant health improvement.

Plants are known to produce defense responses when they are under stress conditions through physical, hormonal and other chemical signaling mechanisms. [8] Physical signals include electrical signals [9] and hydraulic signals. [10] Phytohormones are hormonal signaling molecules that regulate the physiological processes within plants. Other common chemical signaling molecules include volatile organic compounds (VOC), reactive oxygen species (ROS), reactive nitrogen species (RNS) and metabolites. [11] As compared to the detection of physical signals, the dynamic changes and biological significance of chemical signaling molecules in plants are more extensively studied. This approach generates valuable biological insights due to the diversity of chemical signals and their well-studied connections to biological processes.

On the other hand, the rise in environmental pollution, driven by industrialization and human activities such as transportation, poses serious risks to plant health. Environmental toxins, such as organic pollutants and heavy metals, can hinder plant growth when absorbed. [12] Additionally, the extensive use of pesticides in modern agriculture for managing pests can lead to unintended consequences, such as toxicity from excessive residue buildup. [13] The high pesticide residue levels also pose a risk to human health when consumed, raising concerns regarding food safety. [14] The detection of environmental toxins and pesticide residues is therefore crucial to ensure sustainable agricultural production without compromising food quality and safety.

Conventional methods for detection of environmental toxins and chemical signaling molecules of plants, such as gas-chromatography-mass spectrometry (GC-MS), [15-16] high-performance liquid chromatography (HPLC) [17] and rapid bioassays, [18] give precise and comprehensive insights into the chemical information of plants. However, such testing is limited to in-lab settings with time-consuming sample preparation and data processing required, preventing real-time analysis of plants. Additionally, sample preparations for such tests often involve destructive steps such as crushing and purification of samples. [15-16] These destructive procedures prevent the continuous detection of plants' biomarkers in the natural growth status, unable to reveal the dynamic and complex plant signaling network and preventing real-time monitoring. Additionally, the bulky and costly machines further restrict large-scale deployment in agricultural fields, making them less accessible to farmers.

To ensure effective monitoring and timely intervention, non-destructive chemical sensors for in-field detection are being actively developed and explored. Compared to conventional methods such as GC-MS and HPLC, non-destructive chemical sensors prevent extensive tissue damage to plants and thus allow chemical analysis in plant's native status across a wide time span. This information reveals the most genuine responses of plants with temporal dynamics. Furthermore, many non-destructive techniques allow faster detection or even real-time monitoring of chemical biomarkers, due to the elimination of sample preparation. Additionally, such chemical sensors are miniaturized and relatively low-cost, with the potential for deployment in agricultural fields for large-scale monitoring.

In this review, we will introduce non-destructive chemical sensors designed for in-field monitoring of plant health through sensing environmental pollutants, agrochemicals, and plant biomarkers. The recent advancements in materials selection, sensor design and technologies reported are highlighted. Although there are various published reviews for plant monitoring, [19-22] they are often focused on a specific type of biomarkers, such as VOCs, a particular detection method, such as the electrochemical method, or specific types of electrodes, such as microneedles. Therefore, a comprehensive review is needed to explore the broader application of chemical sensing technologies currently investigated for plant monitoring. There is also a lack of clear distinction between fully non-destructive chemical sensors and those that require destructive procedures, such as utilizing plant extracts or supernatant solutions. Here, this review highlights non-destructive sensing methods, covering the most recent developments for each reported analyte, and includes novel detection methods not previously applied to those analytes, with a particular emphasis on flexible and wearable sensors. Additionally, the review will address current challenges and limitations in non-destructive chemical sensing for plant health monitoring. Furthermore, the review will explore prospects for the incorporation of wearable technologies for plant chemical sensing.

2. Sensing devices and techniques

Early developments of non-destructive chemical sensors employ invasive methods that are directly inserted into plant tissues, causing mechanical damage to plants. The monitored signals

obtained through these methods may be affected by the plant's physiological responses to the injury, potentially compromising measurement accuracy. Many researchers therefore explored minimally invasive (e.g. microneedles) and non-invasive sensors. [23] Rigid sensors are unable to achieve high conformability on the surface of plants. This lack of proper attachment not only reduces the accuracy of measurements but also limits the sensor's ability to maintain stable contact over time.

Ms Yi Jing Wong is currently pursuing a Ph.D. with an A*STAR Graduate Scholarship at the School of Materials Science and Engineering, Nanyang Technological University (NTU), Singapore under the supervision of Prof. Xiaodong Chen and Prof. Xian Jun Loh. She obtained her BEng in Materials Science and Engineering from NTU. Her research interest lies in the field of plant-wearable sensors and flexible devices.

Dr Yifei Luo obtained her Ph.D. in Materials Science and Engineering from Nanyang Technological University, Singapore. She is currently a senior scientist at the Institute of Materials Research and Engineering (IMRE), A*STAR, Singapore. Her research focuses on plant-wearable sensors, hydrogels/ionogels, and flexible devices.

Prof. Xian Jun Loh is the Executive Director at the Institute of Materials Research and Engineering (IMRE), A*STAR, Singapore. He is also the current President and member of the Executive Committee of the Singapore National Institute of Chemistry. He specializes in biodegradable thermogels and is highly knowledgeable in developing materials for various applications including biomedical, engineering, cosmetics, personal care and food.

Prof Xiaodong Chen is the Distinguished University Professor at Nanyang Technological University (NTU), Singapore. He is an expert in the areas of flexible materials and devices, nanobiointerfaces, and nanoelectronics. He is the editor-in-chief of *ACS Nano*. He has been elected as a Fellow of the Singapore National Academy of Science and a Fellow of the Academy of Engineering Singapore.

To address these challenges, wearable and flexible sensors, widely used for biomedical applications, [24-25] are explored for on-plant measurements. [20, 26-30] Their flexibility allows them to conform closely to plant surfaces, providing more reliable data and opening new possibilities for real-time, field-based plant health monitoring. Additionally, flexible sensors usually use fewer materials and can potentially be manufactured on a large scale using low-cost processes such as printing. The use of flexible and wearable sensors for plant health monitoring is still a relatively new and growing field, with a focus on developing materials and methods to achieve better sensitivity, selectivity, and stability for in-field detection.

Common recognition elements include enzymes and molecularly imprinted polymers [31] for sensing the target chemical (Figure 1). These allow the sensor to achieve highly specific detection of the chemical molecules. Besides, researchers are exploring various materials, such as nanomaterials [32] and metal-organic frameworks, due to their high surface area and chemical tunability for sensitive and selective chemical detection.

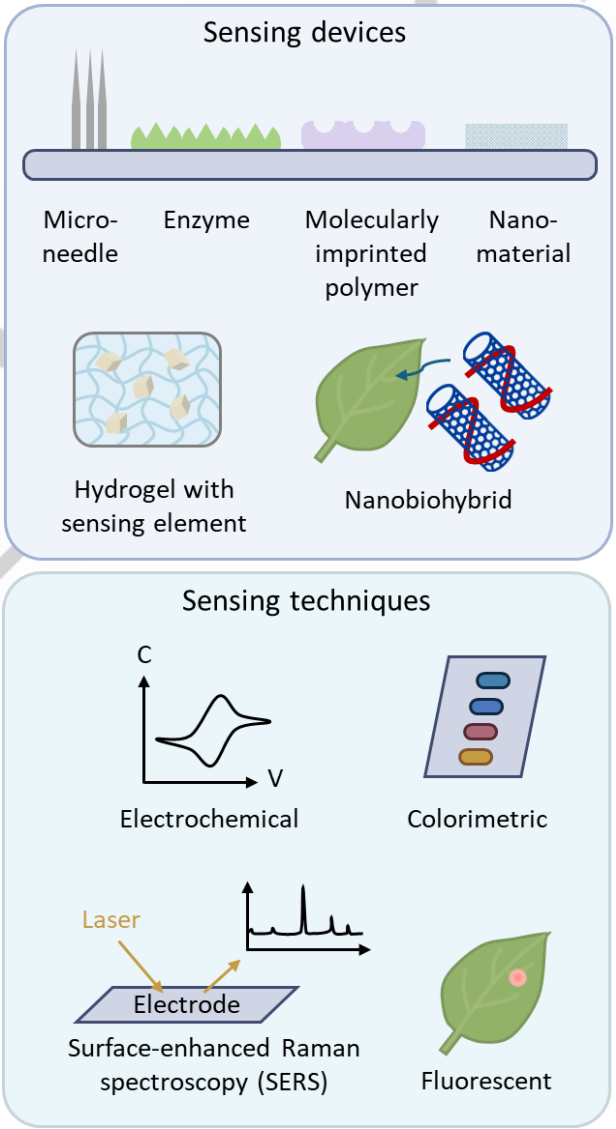

Figure 1: Sensing devices and techniques explored for non-destructive plant chemical sensors.

Another emerging type of sensing device is nanosensors [33] and nanobiohybrids, [34] where nanomaterials are delivered into living plants to performance sensing functions. Nanosensors report the chemical environment within plant tissues through the interaction

of target analytes with nanomaterials. On the other hand, nanobiohybrids endow organisms with new properties that can be used for monitoring environmental chemicals.

Among the various sensing techniques used in non-destructive chemical sensors, electrochemical and optical sensing are emerging methods due to their high sensitivity and selectivity (Figure 1). Electrochemical detection monitors a change in electrical signals when electrochemical reactions occur through the interactions between the target chemical and the electrode surface. These allow the electrode to achieve direct detection of the biomarkers. Detection methods include resistance, cyclic voltammetry (CV), differential pulse voltammetry (DPV), square wave voltammetry (SWV) and amperometry. Optical methods that are utilized for chemical sensing of plant health involve colorimetric sensing, fluorescent sensing and surface-enhanced Raman spectroscopy (SERS).

3. Sensors for various chemicals

3.1. Environmental pollutants and toxins

Climate change has led to an increase in the concentration of ground-level ozone [35], a pollutant known to adversely affect plant health by causing oxidative damage. [36-37] Prolonged exposure to ozone can result in reduced photosynthetic efficiency and cause a decline in overall crop yield. Traditional methods of detecting ozone damage in plants, such as visual identification [38-39] and biochemical assays, [40] are limited by their inability to achieve early detection. To address this limitation, Kim et al. developed a chemical sensor for the identification of ozone damage in plants using a vapour-deposited poly(3,4-ethylenedioxythiophene)-Cl tattoo. [41] The sensor tracks the changes in electrical impedance at high frequencies caused by oxidative damage (Figure 2a). The sensor demonstrated the ability to effectively distinguish ozone damage from drought stress, showing the potential of using electrical impedance spectroscopy for early warning of ozone damage. However, the sensor has not demonstrated its ability to differentiate from other ROS or abiotic stresses. Furthermore, the fabrication process requires optimization to facilitate large-scale applications.

Apart from ozone damage, the presence of environmental toxins can significantly affect the growth of plants, threatening agriculture and food security. [42-43] Common environmental toxins include air pollution, water pollution, soil contamination and climate pollutants. Seker et al. developed a wearable sensor for the detection of atmospheric lead via square wave anodic stripping voltammetry (SWASV). [44] The working electrode comprises a bismuth/Nafion coating with a poly(vinyl alcohol) (PVA) gel as electrolyte carrier (Figure 2b). The sensor achieved detection of atmospheric lead as low as 50 μg L^{-1}. The sensor also showed the ability to resist bending and wind interference. However, the sensor has a short operation duration of 6 hours. Next, Manavalan et al. developed a wearable sensor for the detection of N-(1,3-Dimethylbutyl)-N'-phenyl-p-phenylenediamine (6-PPD) contaminants by CV measurement. [45] The wearable sensor features a sandwich-like structure constructed using a hybrid electrocatalyst, where iron oxide nanocubes were incorporated onto carbon nanotube (CNT) nanoribbons, combined with a gelatin-based hydrogel semisolid electrolyte. The oxidation of 6-PDD for detection is driven by the cleavage of $N\text{-}H_1$ bond, and the presence of OH^- formed in iron oxide helps to reduce the energy barrier of the redox reaction. The detection range of 6-PDD achieved was 100 nM – 18.8 μM with a limit of detection (LOD) of 2.93 nM. The sensor effectively detected 6-PDD on perilla and lettuce leaves, as well as tomato fruit and apple fruits, achieving a high recovery rate of 96.69-97.92%.

In addition, Liang et al. developed a living nanobiohybrid capable of monitoring metal ions and organic pollutants. [46] The living sensor was fabricated by in-situ growth of photoluminescent $[Tb_2(BDC)_3(H_2O)_4]$ metal-organic frameworks (MOFs) inside plants through the immersion of roots in aqueous precursor solutions. The resulting nanobiohybrid was able to achieve a detection range of 0.05–10 μM for pollutants such as Ag^+, Cd^{2+} and aniline through a fluorescence "turn-up" response and for Fe^{3+} and Cu^{2+} through a "turn-down" response when excited by ultraviolet (UV) light. Ligands were added to the MOFs to achieve in-situ MOF formation and fluorescence emission. The organic ligands around the Tb^{3+} absorb the UV lights, and the energy was transferred to Tb^{3+} for luminescence generation. With the presence of pollutants, the luminescent signals undergo quenching for detection. The sensor's high selectivity and sensitivity present a promising solution for monitoring waterborne pollutants. Minimal toxicity was shown in plants incorporated with the MOF nanosensors for 2 weeks. Expanding on the use of nanomaterials for environmental toxin detection, Lew et al. designed fluorescent nanosensors based on single-walled carbon nanotubes (SWCNTs) for real-time monitoring of arsenic pollution. [47] These nanosensors were engineered to detect arsenite—the primary form of arsenic in paddy fields—via alterations in their emission intensity. The SWCNT wrapped with an oligonucleotide sequence containing high contents of guanine and thymine was employed due to the large increase in fluorescence intensity upon detection of arsenite. By integrating the sensors into the leaf mesophyll, the nanosensors identified arsenite absorbed by plants (Figure 2c). Remarkably, after 14 days of application, the sensor demonstrated the ability to detect arsenic concentrations as low as 0.2 ppb.

These nanosensor technologies highlight the potential for real-time, high-sensitivity detection of environmental toxins. However, despite their promising capabilities, current toxicity studies of nanosensors have only evaluated their effects within weeks of application. Long-term studies are essential to assess the ecological and physiological impacts of nanosensors on plants and the environment, ensuring their safe and sustainable use in agricultural systems.

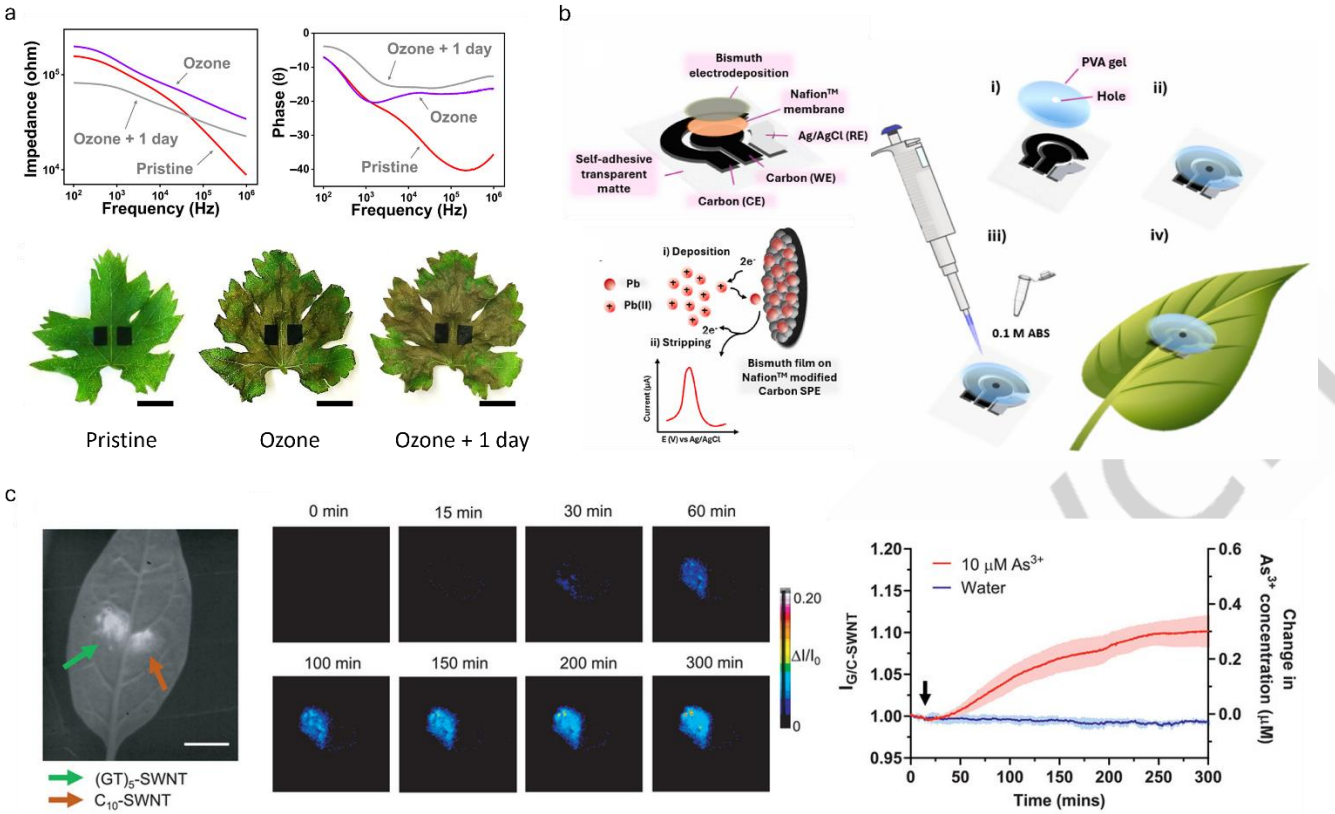

Figure 2: Wearable and portable devices for detection of environmental pollutants and toxins on plants.
(a) Electrochemical impedance measurements using poly(3,4-ethylenedioxythiophene)-Cl for detection of ozone damage on plants. Scale bars: 10 mm:. [41] Adapted with permission from ref [41] Copyright 2020 The American Association for the Advancement of Science. (b) Electrode design with demonstration of lead detection on the left. Sensor placement on plant leaf with PVA gel shown on the right. [44] RE: reference electrode, WE: working electrode, CE: counter electrode, SPE: screen-printed electrode, ABS: acetate buffer solution. Adapted with permission by CC-BY 4.0 license. (c) Bright field image of spinach leaf infiltrated with sensor ($(GT)_5$-SWNT) and control (C_{10}-SWNT) on the left and change in fluorescence intensity of the active sensor upon exposure of 10 μm of arsenite root medium. SWNT: Single-walled carbon nanotube. Adapted with permission from ref. [47] Copyright 2020 Wiley.

3.2. Pesticides

Pesticides are extensively used to regulate the development of crops, such as controlling pests or infestations. However, excessive pesticide residues can result in burns and deformation of plants. [48] Furthermore, the consumption of crops with excessive pesticides can lead to toxicity and carcinogenic effects. [49] To mitigate such risks, regulations were implemented to ensure that residue levels comply with safety limits. Although substantial research has been devoted to developing sensors for monitoring pesticides, most sensors only showed capabilities in monitoring spiked samples and not on-plant monitoring. [50-55] Exploration of methods to monitor pesticide residues non-destructively on plants (Table 1) is therefore essential in ensuring crop safety and environmental sustainability.

Plants have complex and irregular surfaces and are subject to movements and deformations due to environmental disturbances such as wind. Wearable sensors, therefore, require stretchable properties to ensure conformal contact for accurate detection under these conditions. In addition, stretchable properties are required for devices to accommodate plant growth within the monitored period. Zhao et al. fabricated a wearable sensor for monitoring methyl parathion organophosphate pesticide. The serpentine electrode was fabricated via laser-induced graphene (LIG) and modified with an organophosphate pesticide hydrolase enzyme. [56] For detection, an electroactive p-nitrophenol is released when the enzyme hydrolyses methyl parathion. The electrode also demonstrated mechanical stability under 10% strain and achieved a LOD of 2.63 ppb with a rapid response time of 8 minutes. Although enzymatic sensors exhibit high specificity, their stability in complex environmental conditions remains a significant challenge. [57-58] Enzymatic sensors are prone to degradation over time and require specific storage conditions to maintain functionality. [57-58] Further efforts are required to ensure their durability, scalability, and practicality for large-scale agricultural use.

Apart from the detection of organophosphate pesticides, recent advancements have expanded to the monitoring of other pesticide classes, highlighting their potential environmental and health impacts. Paschoalin et al. presented a low-cost sensor, fabricated by screen printing of carbon ink on solution-blown poly(lactic acid) (PLA) for quantification of carbendazim and diquat pesticides. [59] DPV was employed for monitoring carbendazim, while SWV was used for diquat due to the lack of an oxidation peak in DPV measurement. The use of PLA mats in this work improved the electrode sensitivity and repeatability. Teixeira et al. also presented a sustainable solution for monitoring carbendazim and paraquat by employing a biodegradable and flexible cellulose acetate substrate. [60] A wearable double-network hydrogel with embedded composite of dual-shelled upconversion-nanoparticles, zeolitic imidazolate framework and

polydopamine (UCNPs@ZIF@PDA) by Yan et al. achieves real-time and on-site fluorescence detection of 2,4-dichlorophenoxyacetic acid pesticide (Figure 3a). [61] The UCNPs undergo absorption of near-infrared light for upconverting to luminescence. The incorporation of a hydrogel disc allows the sensor to achieve a conformal and adhesive interface with hairy plant surfaces. With the incorporation of image processing methods, the electrode can accurately quantify pesticides with concentrations as low as 20 ng mL^{-1}. The electrode was also able to sustain one-week storage without degradation.

As conventional wearable methods remain limited to surface measurement of pesticides, microneedle SERS patches for the detection of pesticides within agricultural products were explored. The microneedle sensors, composed of Ag nanoparticles and sodium hyaluronate/PVA, allow amplification of Raman signals for accurate detection of thiram and thiabendazole pesticides. [62] By penetrating the cuticle, the microneedles are able to collect pesticide residues both on the surface and inside the leaf. The use of SERS-active Ag nanoparticle substrate results in an improvement of the Raman signal intensity. By employing sodium hyaluronate, the microneedle patch has a high water-absorption capacity, allowing fast collection and detection of pesticide residues. Characteristic Raman peaks of thiram and thiabendazole pesticides were identified and used to accurately monitor residues in spinach and tomato. The detection time required for the sensor was 3 minutes. Additionally, Mohan et al. introduced a flexible polydimethylsiloxane (PDMS)-based SERS substrate for detecting thiram and thiabendazole on fruits, with a lower LOD of 3.20×10^{-11} M and 3.08×10^{-10} M, respectively (Figure 3b). [63] The substrate is made of Ag nanowires from the sandpaper-assisted soft lithography technique. This substrate allows a non-invasive method where it only requires a simple place and peel-off process from the fruit samples for detection. The substrate shows stability over 60 days and is suitable for long-term monitoring. These advancements in enzymatic, fluorescence, and SERS-based technologies provide versatile and scalable solutions for pesticide monitoring, addressing limitations in sensitivity, environmental stability, and usability, thereby enhancing their potential for agricultural and environmental applications.

Apart from conventional wearable sensors placed on plant surfaces, scientists have also extended the monitoring of pesticides via direct contact with fruits and vegetables using glove-integrated sensors. Farshchi et al. fabricated an electrochemical glove sensor based on Ag nano-ink for the detection of Trifluralin pesticide, achieving a LOD of 0.01 µM using DPV and SWV. [64] The Ag nano-ink allows high flexibility for glove application. The peak potential of trifluralin at 0.7 V and 0.3 V for DPV and SWV respectively allows accurate detection using electrochemical response. However, the sensor was only tested on fruit surfaces with prepared pesticide solutions. The ability to selectively detect Trifluralin on plant or fruit surfaces covered with interfering chemicals is essential for real-world application.

In a broader application, Raymundo-Pereira et al. demonstrated the detection of four classes of pesticides (carbamate, phenylamide, bipyridinium and organophosphate) using a carbon-based glove-embedded sensor (Figure 3c). [65] To achieve high selectivity and sensitivity of each pesticide, the sensing layer and detection method were varied. Carbon spherical shells and Printex carbon nanoballs electrodes were employed for carbendazim (carbamate) and diuron (phenylamide), respectively, using DPV. A pre-treated screen-printed electrode (SPE) was employed for the detection of paraquat (bipyridium) and fenitrothion (organophosphate) using SWV. This non-enzymatic glove-embedded sensor achieves effective discrimination of the 4 pesticides, expanding its potential for detecting a broader range of pesticide types. Such glove-based sensors provide a portable, user-friendly platform for on-site pesticide monitoring, offering significant potential for agricultural, environmental, and food safety applications.

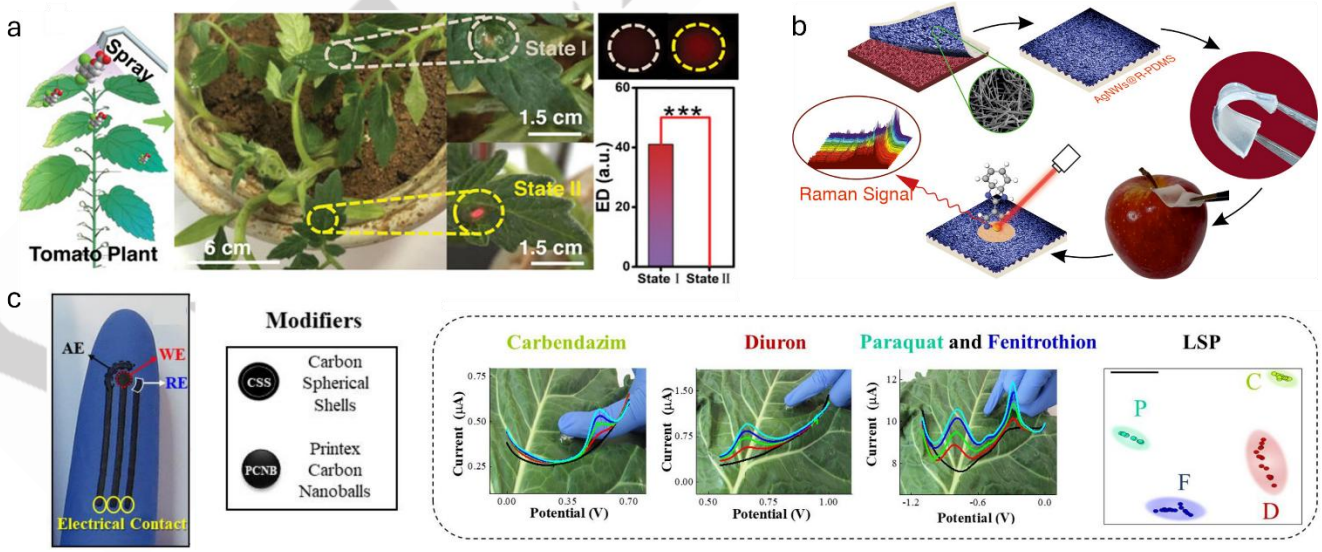

Figure 3: Wearable and portable devices for detection of pesticide residues on plants.
(a) Hydrogel disk response with and without the presence of 2,4-dichlorophenoxyacetic acid pesticide. [61] ED: Euclidean distance. Reproduced with permission from ref [61] Copyright 2024 Wiley. (b) Flexible SERS sensor attached on apple for detection of thiram and thiabendazole pesticide. [63] Reproduced with permission from ref [63] Copyright 2024 American Chemical Society. (c) Wearable glove sensor for on-site detection and classification of four classes of pesticides. [65] AE: auxiliary electrode, RE: reference electrode, WE: working electrode. LSP: Least Square Projection, C:carbendazim, D: Diuron, P: paraquat, F: fenitrothion. Adapted with permission from ref [65]. Copyright 2021 Elsevier.

Table 1: Detailed performance of devices for detection of pesticide molecules on plants.

Detected pesticide	Sensing material	Detection method	Detection range and limit	Plant/sample	Ref
Methyl parathion organophosphate	LIG modified with organophosphorus hydrolase enzyme	CV	20–500 µM LOD: 0.01 µM (2.63 µg L^{-1})	Spinach plant, Apple fruit	[56]
Carbendazim, diquat	Screen-printed carbon ink on solution blown PLA mat	DPV, SWV (selectivity)	0.1–1.4 µM LOD: 43 nM (carbendazim), 57 nM (diquat)	Apple fruit, Cabbage leaves	[59]
Carbendazim, paraquat	Screen-printed carbon ink on cellulose acetate substrate	DPV (carbendazim), SWV (paraquat)	0.1–1.0 µM LOD: 54.9 nM (carbendazim), 19.8 nM (paraquat)	Tomato fruit, Lettuce leaves	[60]
2,4-dichlorophenoxyacetic acid	Embedded dual-shelled UCNPs@ZIF@PDA composite in double-network hydrogels	Fluorescent,	0.02–100 µg mL^{-1} LOD: 20 ng mL^{-1}	Tomato plant, Apple juice, Pear juice, Tap water	[61]
Thiram, thiabendazole	Ag/HA/PVA microneedle patch	SERS	10^{-7}–10^{-4} M (Thiram), 10^{-8} –10^{-5} M (Thiabendazole)	Tea leaf, Spinach, Tomato samples	[62]
	AgNW	SERS	0.1 nM – 1 mM LOD: 3.20 × 10^{-11} M (Thiram), 3.08 × 10^{-10} M (Thiabendazole)	Apple fruit	[63]
Trifluralin	Ag nano-ink	DPV and SWV	0.01 µM – 1 mM LOD: 0.01 µM	Tomato fruit, Mulberry leaves	[64]
Carbendazim, diuron, paraquat, fenitrothion	Carbon electrodes, coated with carbon spherical shells or printex carbon nanoballs	DPV (carbendazim, diuron) SWV (paraquat, fenitrothion)	0.1–1, 1–10, 0.1–1, 1–10 µmol L^{-1} respectively LOD: 4.7 ×10^{-8}, 9.2 × 10^{-7}, 2.4 × 10^{-8}, 6.4 × 10^{-7} mol L^{-1} respectively	Cabbage leaves, Apple fruit, Orange juice	[65]

LIG: Laser-induced graphene; PLA: polylactic acid; UCNPs@ZIF@PDA: upconversion-nanoparticles@zeolitic imidazolate-framework@polydopamine; HA: hyaluronic acid; PVA: polyvinyl alcohol; AgNW: Silver nanowire; CV; cyclic voltammetry; DPV: differential pulse voltammetry; SWV: square wave voltammetry; SERS: surface-enhanced Raman spectroscopy; LOD: limit of detection.

3.3. Phytohormones

Phytohormones are one of the most important regulators that affect the physiological processes within plants. [66-67] Common phytohormones include auxins, salicylic acid (SA), gibberellins (GA), abscisic acid (ABA), and jasmonic acid (JA). In addition to these non-volatile phytohormones, the monitoring of volatile phytohormones, such as ethylene and methyl jasmonate (MeJA), has also been explored (Table 2). The production of phytohormones is tightly regulated by plant development status and environmental conditions. [66] When plants are subjected to biotic or abiotic stresses, phytohormones help to trigger adaptive defense responses to prevent adverse effects on plant growth and development. [68] Monitoring phytohormone levels in plants provides valuable insights for optimizing and regulating their growth processes.

Auxins affect changes in plant cell development and are important growth regulators, [69-70] while SA participates in defense signalling and enhances plants' defense responses. [71] Sun et al. demonstrated the measurements of indole-3-acetic acid (IAA) auxin and SA by electrochemical detection using a paper-based analytical device with a disposable stainless steel electrode. [72] However, this method is destructive as it requires measured plants to be cut and placed on the device before electrochemical detection can be conducted. To reduce the mechanical damage to plants, his team further developed a microneedle electrode for continuous monitoring of IAA and SA. [73] The stainless steel microneedle was coated with carbon cement and multi-walled carbon nanotubes (MWCNTs) to enhance the sensing capabilities by increasing the number of active sites and facilitating the electron transfer kinetics. This modification may also be the reason for the good selectivity of the sensor against other phytohormones, due to hydrogen bonding or electrostatic interactions with IAA and SA. Following which, Bukhamsin et al. reported a real-time and long-term monitoring of foliar IAA and SA by employing superparamagnetic iron(III) oxide (Fe_3O_4) nanoparticles intercalated with MWCNT as coating on a magnetized microneedle. [74] The sensor selectivity was also evaluated using other phytohormones at a concentration of 1 mM, showing minimal overlap in oxidation potentials. In this work, a multipulsed amperometric (MPA) detection was used to reactivate the carbon-based electrode between measurement events to extend the longevity of the sensor. The use of MPA have shown to maintain strong linear correlation detection of both IAA and SA over a range of 5–150 µM, with a LOD of 1.41 µM for IAA and 1.15 µM for SA. An in-vivo test of the sensor on plants showed a minimum lifetime duration of 25 hours. The sensor was used to study the effect of light on IAA and SA, revealing diurnal oscillations, age-dependent changes in older leaves of flowering tobacco plants and responses to extended photoperiods. The sensor was also able to monitor the rise in foliar IAA and SA levels 3 hours post-pathogen infection. Next, Zhang et al. developed a carbon-based gel electrolyte, CNT@Cu-Tannic acid, for the detection of IAA. [75] CNT was incorporated to improve the electrical conductivity, and tannic acid was added to improve the adhesion strength on the plant surface. Glycerol was introduced into the gel electrolyte to increase water retention for up to 15 days. By CV measurement, the electrolyte-based sensor has a LOD of 10.9 µM. Also, Ang et al. demonstrated a nanosensor that can monitor synthetic auxins, 1-naphthaleneaceticacid (NAA) and 2,4-dichlorophenoxyacetic acid (2,4-D) using corona phase molecular recognition (Figure 4a). [76] The corona phase is achieved by wrapping amphiphilic polymers around SWCNTs, allowing selectivity towards auxin analytes. The binding of the analytes causes fluorescence quenching response, triggering a change in the fluorescence intensity which can be monitored optically. [76] The sensor requires a detection time of 10 minutes with a LOD of 8.2 µM for NAA and 0.35 µM for 2,4-D. Notably, nanotoxicity remains a concern for long-term applications even though the nanosensors have been shown to remain stable 7 days post-infiltration.

ABA plays a pivotal role in inhibiting plant growth and regulating stomata opening when plants experience environmental stresses. [77] For in-situ detection of ABA, microneedle designs are currently employed. Li et al. prepared a microneedle sensor array based on gold (Au) and tin(IV) oxide (SnO_2) nanoparticles with vertical graphene nanosheets. [78] The electrode was able to detect ABA via amperometric response due to the presence of direct catalytic oxidation mechanism of the electrode. The fast electron transport using vertical graphene allows high sensitivity of the electrode. A LOD between 0.002 and 0.005 µM over a pH range of 4-7 (typical range of *in vivo* pH in plants) was achieved, and the sensor exhibited high selectivity against nine other interfering species.

For the monitoring of SA levels, LIG electrodes have been utilized to detect changes in the CV oxidation peaks of SA with the help of machine learning for SA identification. [79] However, the study only employed measurements on the extracted solutions of lettuce and not on real samples. Furthermore, the study did not assess the selectivity of the electrodes in the presence of other phytohormones or small molecules. To address this, Perdomo et al. integrated a reverse iontophoresis system with a LIG electrode to achieve non-destructive measurement with enhanced selectivity (Figure 4b). [80] The reverse iontophoresis system enables non-invasive extraction of plant liquids based on the use of cationic and anionic hydrogels between the electrode and the plant. This approach achieved a short extraction time of 20 seconds and accurately tracked drought and salt stress in plants with elevated SA levels. Additionally, Nejad et al. modified LIG electrodes with Nafion, leveraging its cation exchange properties for continuous monitoring of SA. [81] Although this modification led to a reduced sensitivity and a higher LOD of 1.44 µM, it provided higher stability for continuous monitoring. In a different approach, Bukhamsin et al. utilized magnetic molecularly imprinted polymer (MIP) in a microneedle design for SA detection. [82] Methacrylic acid was chosen as the monomer for its ability to form hydrogen bonds with SA while Fe_3O_4 nanoparticles were incorporated to confer magnetic properties. The magnetic nature allows selective attachment of the MIP onto the working electrode. The MIP can then bind with SA for detection via electro-oxidation. The sensor achieved real-time monitoring of SA using CV and SWV characterization, with a LOD of 2.74 µM. The sensor also displayed the ability to detect fungal infection in tobacco plants within 5 minutes of inoculation.

JA is a critical regulator involved in plant stress and developmental pathways, including root growth, plant germination and fruit ripening. [83] Under pathogen attack, JA levels increase to activate the pathogen-related stress response. However, an elevated concentration of JA often leads to slower growth, such as a decrease in plant height and biomass. [84] Larrieu et al. presented a fluorescent sensor for monitoring local and long-distance responses of JA. [85] By utilizing JAZ proteins which undergo degradation in response to JA, the biosensor comprised AtJAZ9 proteins with fusion of VENUS variant of yellow fluorescent protein. Quantitative measurement along with response mapping of JA was achieved using confocal microscopy

Lastly, ethylene is a phytohormone that plays a key role in regulating plant development and is commonly used to evaluate fruit ripeness and plant flowering. It is found that the production of ethylene is readily influenced by biotic **[86-87]** and abiotic **[88]** stresses. Hossain et al. developed a real-time plant wearable for the simultaneous measurement of ethylene and SA (Figure 4c). [89]. Apart from monitoring the phytohormones, it has incorporated the ability to monitor plant growth and the microclimate environment such as temperature and humidity. The ethylene and SA sensors were coated with copper complex-carbon nanotube (CNT) and copper MOF-carbon black-Nafion respectively as the sensing element. Copper complex (I) forms a second complex when bound with ethylene, restricting interaction with the SWCNT and decrease in current, allowing detection of ethylene via CV, with a LOD of 0.6089 ppm. On the other hand, DPV measurement allows the detection of SA with a LOD of 0.644 µM. The sensor showed high selectivity against interfering species and even their mixtures. It also displayed the ability for more than 60 days of monitoring. Investigating the spatial and temporal patterns of water transport and signaling of ethylene and SA showed a high correlation, bringing about the possibility of early stress detection. Next, a tattoo plant wearable fabricated from graphene with copper composite-CNT as the sensing material allows direct sensing on leaves. [90] Due to the reduction in resistance of SWCNT upon ethylene interaction, the resistance of the sensor was monitored for analyte detection. Monitoring of ethylene emission of plants under combined stresses was achieved with the sensor, with a LOD of 0.13 ppm. An oxide semiconductor chemiresistor was proposed by Jeong et al. for assessing food ripening via ethylene emission. [91] The sensor employs SnO_2 material with a chromium(III) oxide (Cr_2O_3) coating for high selectivity towards ethylene gas. SnO_2 materials are sensitive to ethylene and triethylamine. The bilayer design therefore allows catalytic oxidation of interfering gases into carbon dioxide and water without sacrificing the transport of ethylene. The sensor achieves a LOD of 24 ppb. However, a high sensor temperature of 375 °C is required for optimal sensing of ethylene in this system. Separately, Liu et al. fabricated a screen-printed MXene-reduced palladium nanoparticle-based wireless plant wearable device for continuous monitoring of ethylene (Figure 4d). [92] The incorporation of Pd nanoparticles improves the adsorption of ethylene on the surface of the electrode. Upon absorption of ethylene molecules, the inter-flake spacing increases due to the presence of ethylene intercalants, causing an increase in inter-flake resistance. The wireless radio frequency (RF) sensor tags on the electrodes allow continuous monitoring of ethylene emission over 8 days, with a LOD of 0.84 ppm.

3.4. Volatile organic compounds

Volatile organic compounds (VOCs) are emitted by plants in response to abiotic and biotic stress factors. [93] These compounds play crucial roles in regulating physiological processes and mediating interactions with the environment. For instance, VOCs facilitate pollinator attraction [94] and serve as signaling molecules to neighboring plants under environmental stress. [95] Additionally, VOC emissions often represent a direct response to stress conditions, reflecting changes in plant metabolism and strategies. [96] Common VOCs include terpenoids, alcohols and sulfur-containing compounds. [97] Conventional methods for detecting VOCs, such as gas chromatography techniques, are time-consuming where substantial sample preparations are required, preventing real-time monitoring. Furthermore, bulky equipment with high costs prevents large-scale application in fields. To

address these challenges, portable and wearable devices are being developed (Table 3).

Methanol, a VOC product of metabolism, is emitted through plants during defense against insects or wounding. [98] The production of methanol is also affected by environmental conditions such as temperature, light and water status. [99] The monitoring of methanol is therefore important as it provides valuable health information about the growth of plants. A three-arm carbon electrode printed on a polyethylene terephthalate (PET) substrate was fabricated by Ibrahim et al. for the selective detection of methanol. [100] The sensing electrode consists of a conductive polymer (poly(2-amino-1,3,4-thiadiazole)) modified with platinum (Pt) nanoparticles for electrochemical oxidation of methanol, with Nafion infused into the pores of the carbon electrode as polymer electrolyte. The influence of humidity was reduced with a filter membrane and the concentration of methanol was monitored using CV measurements. The sensors achieve a detection range of 0.5-500 ppm with a response time of 10 s. The difference in methanol concentration was recorded between the two genotypes of maize plants. Under infection or disease, plants often release specific VOCs via their defense mechanism. [101] Monitoring such disease-specific VOCs provides a non-invasive approach to detect and diagnose plant diseases, [102] allowing for early mitigation and management.

A chemiresistor was fabricated by Zheng et al. to detect monoterpene α-pinene VOC released from *Platycladus orientalis* plants to determine drought stress and mechanical damage. [103] The chemiresistor consists of a Au interdigital electrode printed on a PET substrate, and the sensing element is a composite material of polyethylene-co-vinyl acetate (PEVA)/MWCNT. [103] By utilizing the percolation threshold of the composite material, where a large decrease in electrical conductivity can be recorded when a specific concentration of the filled particles is obtained, the sensor was able to have a LOD of 0.5 ppm and a short recovery time of 8 s. The sensor also displayed stable results over a wide humidity range of 40-90%. Surprisingly, the sensor demonstrated good selectivity when exposed to higher concentrations of other plant VOCs. The sensor was also integrated with an NFC tag to allow monitoring on smartphones. Although the electrode demonstrated real-time monitoring capabilities, the plants were kept in an enclosed environment during the detection period, which is not representative of real-world conditions. Next, titanium dioxide (TiO_2) and SnO_2 modified SPE were explored by Fang et al. for the detection of p-ethylguaiacol, a VOC signature for plants infected with *Phytophthora cactorum* fungus. [104] The concentration of p-ethylguaiacol can be monitored by CV and DPV measurements, achieving a LOD of 35 nM for TiO_2 modified electrode. It should be noted that the electrode experiences a loss in activity and has not shown good stability over time.

To ensure a holistic and accurate detection of different biotic or abiotic stresses of plants, sensors with the capability to monitor multiple VOC profiles are being developed. Li et al. developed a reduced graphene oxide (rGO)-based sensor for real-time monitoring of the VOC profile on plants. [105] The rGO sensor was functionalized with Au nanoparticles or chemical ligands to allow the formation of hydrogen or halogen bonding with VOCs (Figure 5a). The sensor detects VOCs through the change in resistance upon VOC interaction with sensors and has a LOD between 0.13 and 1.4 ppm. The sensor with 8 sensing elements successfully identified Phytophthora infection (leading to late blight) in tomato leaves within 4 days after inoculation. The sensor was able to quantify 13 VOC profiles at 10 ppm, including two late blight markers, with a high classification accuracy of >97%. However, it is noted that calibrations are needed to minimize effects of temperature and humidity. This complicates the use of the sensor for in-field applications due to the dynamic environment which requires extensive calibration. Next, Lee et al. developed an electrode with hybrid network of gold and silver nanowire (Au@AgNW) with MWCNT (Figure 5b). [106] The sensing materials were embedded in a hydrophobic and gas-permeable sol-gel layer to prevent interference from water. The Au@AgNW electrodes were coated with fluorothiophenol and chlorothiophenol ligands to detect ketone and aldehyde-based VOCs through halogen bonding. The electrical resistance changes upon the attachment of VOC molecules. The electrode was incorporated with microclimate (temperature, humidity) sensors and has been shown to detect pathogen infection within 4 days of inoculation. To enable real-world applications, Lee et al. highlighted miniaturization and flexibility as critical advancements for the next generation of multimodal sensors.

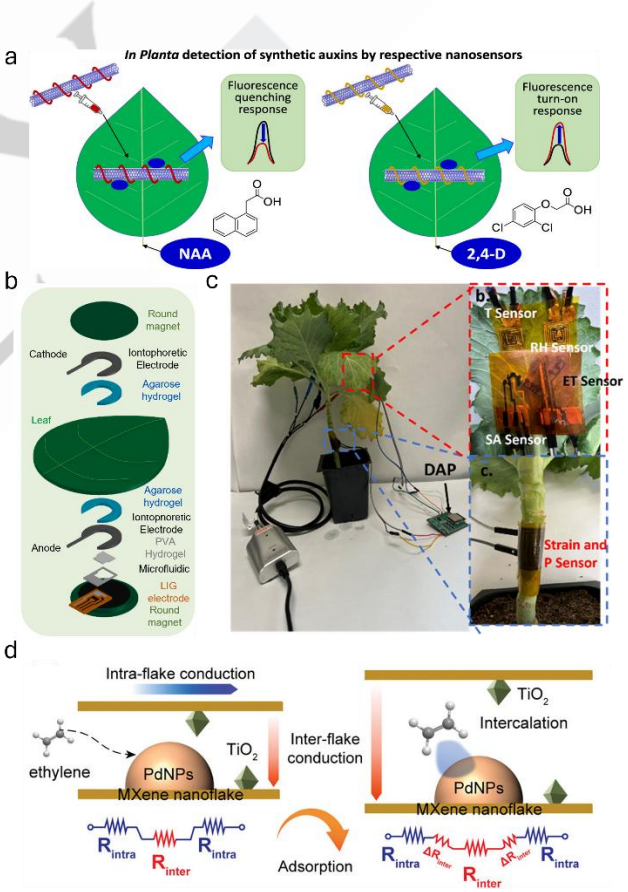

Figure 4: Nanosensors and portable devices for detection of phytohormones. (a) Nanosensor based on corona phase molecular recognition with fluorescent quenching response upon binding with auxin analytes. [76] Reproduced with permission from ref [76] Copyright 2021 American Chemical Society. (b) Sensor with reverse iontophoresis to improve extraction of plant liquids. [80] Adapted with permission from ref [80] Copyright 2024 Elsevier. (c) Sensor with the ability to monitor SA, ethylene (ET), relative humidity (RH), temperature (T), strain and pressure (P) through the data acquisition and processing module (DAP). [89] (d) Changes in inter-flake conduction in MXene nanoflake with Pd nanoparticle for detection of ethylene. [92] Reproduced with permission from ref [92] Copyright 2023 Wiley.

Table 2: Detailed performance of sensors for phytohormones in plants.

Detected phytohormone	Sensing material	Detection method	Detection range and limit	Plant/sample	Ref
IAA, SA	Stainless steel microneedle	DPV	0.1–20 µM	*Arabidopsis thaliana*	[73]
	Magnetized microneedles coated with Fe_3O_4 intercalated MWCNT	SWV, MPA	5–150 µM LOD: 1.41 µM (IAA), 1.15 µM (SA)	*Arabidopsis thaliana* Tobacco (*N. benthamiana*)	[74]
IAA	CNT@Cu-Tannic acid hydrogel electrolyte	CV	20–300 µM LOD: 10.9 µM	Cherry tomato plant	[75]
Synthetic auxins (NAA and 2,4-D)	Amphiphilic polymers wrapped with SWCNT	Fluorescent, image processing	LOD: 8.2 µM (NAA), 0.35 µM (2,4-D)	Spinach plant, *Arabidopsis thaliana*, Pak Choi plant (*Brassica rapa subsp. Chinensis*), rice (*Oryza sativa*)	[76]
ABA	Au@SnO2-vertical graphene microneedle	Amperometric	0.012 (or 0.024)–495.2 µM LOD: 0.002 and 0.005 µM	Arabidopsis seedlings (pH 6.2), grapes (pH 4.5), radishes (pH 5.2)	[78]
SA	LIG with reverse iontophoresis	CV	10–1000 µmol L^{-1} LOD: 8.2 µmol L^{-1}	Avacodo (*Persea americana Hass*)	[80]
	LIG with Nafion	CV, SWV	6.6–200 µM LOD: 1.44 µM	Aloe vera plant (*Aloe barbadensis*), Philodendron brasil plant (*philodendron hederaceum*)	[81]
	Magnetic Fe_3O_4 incorporated MIPs MIP: MAA	CV, SWV	2.74–150 µM	Tobacco	[82]
JA	AtJAZ9 protein with VENUS variant of fluorescent protein	Fluorescent	-	*Arabidopsis thaliana*	[85]
Ethylene, SA	Copper complex-SWCNT (Ethylene) Copper MOF-Carbon black-Nafion (SA)	CV (Ethylene), DPV (SA)	0.1–115 ppm (Ethylene), 0.1–1000 µM (SA) LOD: 0.6089 ppm (Ethylene), 0.644 µM (SA)	Bell pepper plant, Tomato plant	[89]
Ethylene	Copper complex-SWCNT on graphene	Resistance	0.1-115 ppm LOD: 0.13 ppm	Bell pepper plant	[90]
	SnO_2 with Cr_2O_3 coating	Resistance	0.1–2.5 ppm LOD: 24 ppb	Fruits (Banana, Peach, Kiwi, Apple Mango, Blueberry)	[91]
	Screen-printed MXene@Pd nanoparticles	Resistance	0.5–5, 5–20 ppm LOD: 0.084 ppm	Fruits (Apple, Banana, Mango, Kiwi),	[92]

IAA: indole-3-acetic acid; SA: salicylic acid; NAA: 1-naphthaleneaceticacid; 2,4-D: 1-naphthaleneaceticacid; ABA: abscisic acid; JA: Jasmonic acid; SWCNT: single-walled carbon nanotube LIG: Laser-induced graphene; MIP: molecular imprinted polymer; MAA: methacrylic acid; MOF: metal-organic framework; DPV: differential pulse voltammetry; SWV: square wave voltammetry; MPA: multi-pulsed voltammetry; CV; cyclic voltammetry; LOD: limit of detection.

To realize real-world monitoring of plants, Wang et al. developed an extrusion-printed colorimetric sensor array that allows VOC profiling. [107] The colorimetric sensor uses gas-sensitive dyes encapsulated in MOFs to detect specific VOCs (Figure 5c). The incorporation of dyes in MOF with porous nanostructure increases the surface area and improves the VOC adsorption. A hybrid ink for extrusion printing was fabricated by mixing the powdered dyes and MOFs with hydrophobic PDMS. The use of a PDMS layer as the surface coating also prevents humidity influence and improves the sensitivity of the electrode. The nine-element sensor array was able to discriminate 8 different VOCs with a LOD of 1 to 0.5 ppm and a response time of 20 minutes. With the use of extrusion printing during the fabrication process, high scalability can be achieved. Furthermore, the sensor can sustain stretching up to 50% strain and is not affected by mechanical twisting or bending (Figure 5d). In real-world scenarios, the sensor was able to achieve in-situ monitoring of the VOC from wheat leaves, with early detection of wheat scab within 2 days of inoculation. However, the colorimetric sensor is limited to single-use applications and cannot be reused for repeated detection.

Lastly, Choi et al. achieved real-time monitoring of multiple VOCs' profiles, such as nicotine, methanethiol, airborne thiram, phenethylamine, by incorporating nanosensors into various living plants for SERS detection. [108] The nanosensor is constructed using thiolated silica nanoparticles with Ag bumpy nanoshells (AgNS), which amplify Raman scattering in the near infra-red range, allowing for label-free detection of multiple molecules. The nanoparticles are appropriately sized to traverse stomatal openings while remaining confined within the intracellular matrix. The surface of AgNS was wrapped with water-soluble polymers to improve the colloidal stability of the nanoparticles. Additionally, functional polymers capable of interacting with target analytes can be employed to broaden the range of detectable molecules. The nanosensor obtains a detection range of 10 ppt–100 ppb. The nanobionic sensor plant can accurately detect VOCs emitted by neighboring wounded plants of a different species. The nanosensor plant has also demonstrated the ability to detect fungal infection in strawberries 3 days post-infection, and 1 day before any visual symptoms were observed. Using living plants as sensors offers various benefits, including high sensitivity for multi-modal detection and reduced need for external power sources. However, to ensure reliable performance, it is important to understand how the complex plant environment may influence SERS signals. Additionally, specificity can be compromised when nanosensor plant and target plant emit similar VOCs, making it essential to account for overlapping chemical profiles.

Monitoring plant VOCs is crucial for understanding changes in plant health and development. However, significant challenges remain in monitoring VOCs with high sensitivity and selectivity. Future research should focus on developing sensor arrays capable of effectively differentiating complex VOC profiles. Additionally, fabrication techniques should prioritize miniaturization and the adaptability of sensors to accommodate plant growth. Finally, the long-term selectivity, stability, and repeatability of sensor arrays must be optimized for practical applications.

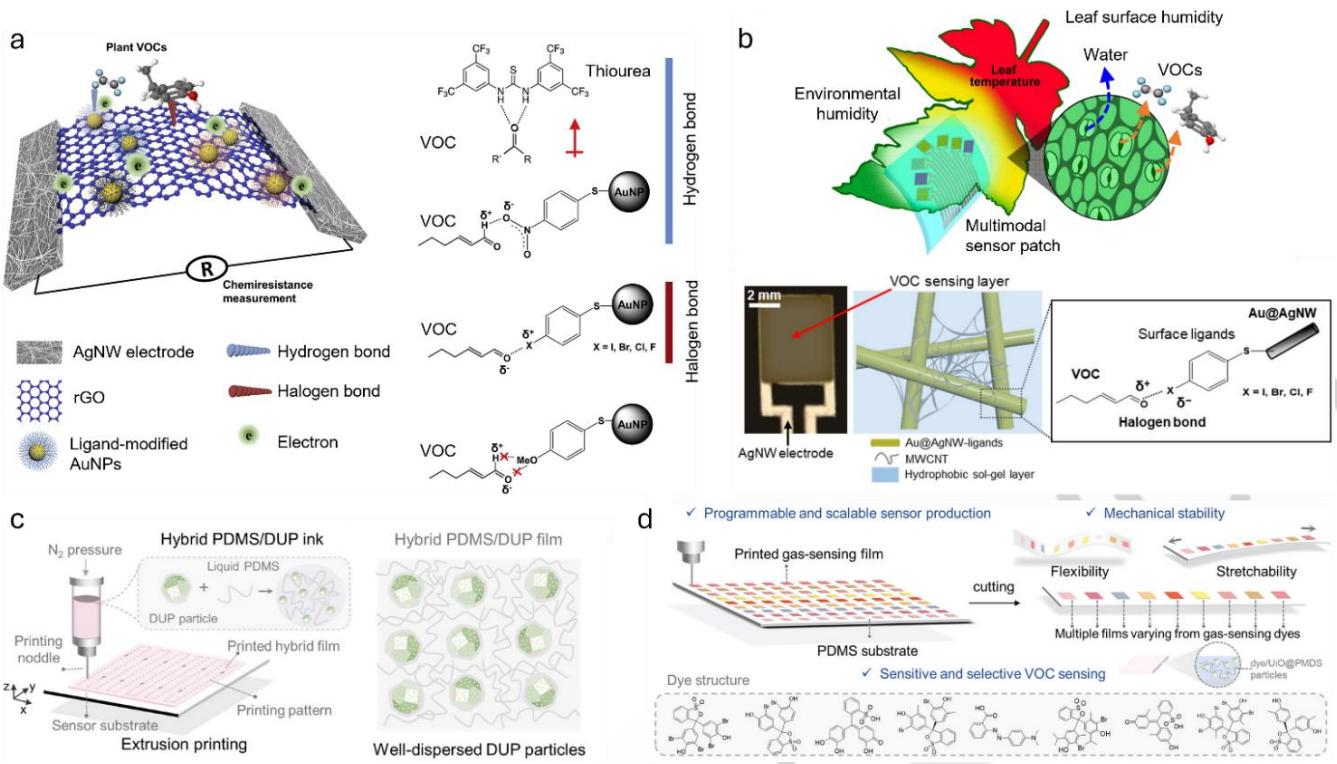

Figure 5: Wearable and portable devices for detection of volatile organic compounds emitted by plants.
(a) rGO-based sensor was functionalized with Au nanoparticles for the detection of VOCs through hydrogen or halogen bonding. [105] Adapted with permission from ref [105] Copyright 2021 Elsevier. (b) Au and Ag nanowire hybrid for monitoring VOC was incorporated with humidity and temperature sensors. [106] Reproduced with permission from ref [106] Copyright 2023 The American Association for the Advancement of Science. (c) Fabrication of colorimetric sensor by extrusion printing using hybrid PDMS/DUP ink, prepared from mixing the powdered dye, UIO-66 metal-organic framework with PDMS particle with liquid PDMS. [107] (d) Colorimetric VOC sensor with flexible and stretchable properties. [107]

Table 3: Detailed performance of sensors for volatile organic compounds emitted by plants.

Detected VOC	Sensing material	Detection method	Detection range and limit	Plant/sample	Ref
Methanol	Conductive polymer (poly(2-amino-1,3,4-thiadiazole)) modified with Pt nanoparticles	CV, chronoamperometry	0.5–500 ppm	Maize plant	[100]
α-pinene	PEVA/MWCNT	Resistance	1–40 ppm LOD: 0.5 ppm	*Platycladus orientalis* plant	[103]
p-ethylguaiacol	TiO_2 or SnO_2 nanoparticle	CV, DPV	0.2 μM – 0.1 mM, 0.6 μM – 0.17 mM LOD: 35 nM	Simulated real fruit plant volatile mixture	[104]
13 VOC profiles	rGO functionalized with Au nanoparticles or chemical ligands	Resistance	10–50 ppm LOD: 0.13–1.4 ppm	Tomato plant	[105]
Ketone and aldehyde-based VOC	Au@AgNW with ligands	Resistance	100–500 ppm	Tomato plant (cv. Mountain Fresh Plus)	[106]
8 VOC profiles	Composite with VOC-sensitive dye, MOFs	Colorimetric	LOD: 0.5–1 ppm	Wheat plant	[107]
Nicotine, phenethyl isothiocyanate, methanethiol, airborne thiram, phenethylamine	Ag bumpy nanoshells on thiolated silica nanoparticles, modified with PDDA, PVA and PAA	SERS	10 ppt – 100 ppb	White clover (*Trifolium repens*), watercress (*Nasturtium officinale*), tobacco (*N. tabacum*). strawberry (*Fragaria x ananassa*, cultivar "Seolhyang"), coriander (*Coriandrum sativum*), rose geranium (*Pelargonium graveolens*), applemint (*Mentha Suaveolens*)	[108]

VOC: volatile organic compounds; PEVA: Polyethylene-co-vinyl acetate; MWCNT: multi-walled carbon nanotube; SPE: screen-printed electrode; rGO: reduced graphene oxide; AgNW: silver nanowire; MOFs: metal-organic frameworks; PDDA: poly(diallyldimethylammonium chloride); PVA: poly(vinyl alcohol); PAA: poly(acrylic acid); CV; cyclic voltammetry; DPV: differential pulse voltammetry; SERS: surface-enhanced Raman spectroscopy; LOD: limit of detection.

3.5. Reactive oxygen species

Reactive oxygen species (ROS) are chemically reactive molecules and are by-products of metabolites. ROS acts as signaling molecules which help to sense and activate responses to biotic or abiotic stress in plants. In particular, hydrogen peroxide (H_2O_2) is one of the most investigated signaling molecules due to its stable and diffusible properties compared to other ROS, such as the hydroxyl radical. Under stress environments, ROS are produced and accumulated to activate the defense response. Conventional ROS sensing methods such as mass spectroscopy

and chemiluminescence assays, are time-consuming and complex, preventing real-time monitoring. H_2O_2 are also widely monitored with fluorescence probes [109], but many suffer from difficulty in quantifying the signals. [110]. Recently, there has been a rising shift towards electrochemical sensors which incorporate nanomaterials and biologically encoded sensors for detection. Furthering the advancement of using corona phase molecules for auxin recognition [76], Lew et al. fabricated a H_2O_2-selective deoxyribonucleic acid (DNA)-wrapped SWCNT as optical sensors for the detection of H_2O_2. [111] A pair of DNA-wrapped SWCNT probes in tandem was used, with one being the reference invariant to H_2O_2. The sensors allow monitoring of both the production and decay profile of H_2O_2 when plants are subjected to wounding. Yao et al. developed a wearable molybdenum disulfide (MoS_2) paper-based sensor for the electrochemical detection of H_2O_2. [112] To enhance catalytic activity, the sensor was coated with Au and Pt nanoparticles. This amperometric detection method enabled a broad detection range, from 0.05 to 3.15 mM, with a low LOD of 0.01 mM. The sensor showed high anti-interference performance against common plant metabolites, but the specificity to H_2O_2 among other ROS was not tested. Parrilla et al. introduced a paper-based hollow microneedle sensor design for in-situ profiling of H_2O_2 (Figure 6a). [113] The sensor incorporates a 3D-printed microneedle and SPE, facilitating simple, low-cost fabrication with high scalability. The paper-based sensor facilitates easy collection of plant fluids for chemical profiling. Next, Zhang et al. demonstrated implantable LIG electrodes powered by an integrated photovoltaic module. [114] Nafion and Pt nanoparticles were added to the LIG electrodes as the anti-interference and sensing layer, respectively. By CV measurements, the concentration of H_2O_2 can be monitored by the change in current.

Recently, Wen et al. employed the use of microfiber-shaped organic electrochemical transistors (fOECTs) for minimally invasive monitoring of H_2O_2. [115] Poly(3,4-ethylenedioxythiophene):poly(styrene sulfonate) (PEDOT:PSS) fibre was used as the channel with flexible Au microfiber functionalized with Pt nanoparticles as the electrochemical gate. By Faradaic reaction at the gate, the OECT can monitor the concentration of H_2O_2. Recognizing that point measurements fail to capture the temporal variation of chemical responses, Coatsworth et al. developed a sensor system designed for detection in the entire plant root environment (Figure 6b). [116] The amperometric sensor was able to monitor the concentration of salt, pH and H_2O_2. In particular, the H_2O_2 sensor uses Prussian-blue mediated carbon as the working electrode and carbon as the counter electrode (Figure 6b). The electrode system has demonstrated the ability to monitor H_2O_2 in real-time with the potential for high-throughput study. However, the sensor still faces challenges in maintaining system hydration to prevent signal drift. Additionally, the current setup is limited to small plants and is difficult to apply to mature plants grown in soil conditions.

3.6. Reactive nitrogen species

In addition to ROS, reactive nitrogen species (RNS) are key signaling molecules that help to regulate various processes within plants. [117-118] As compared to ROS, RNS are less extensively studied, and the precise biological mechanisms are still being explored. Common RNS include nitric oxide, nitrogen dioxide and ammonia.

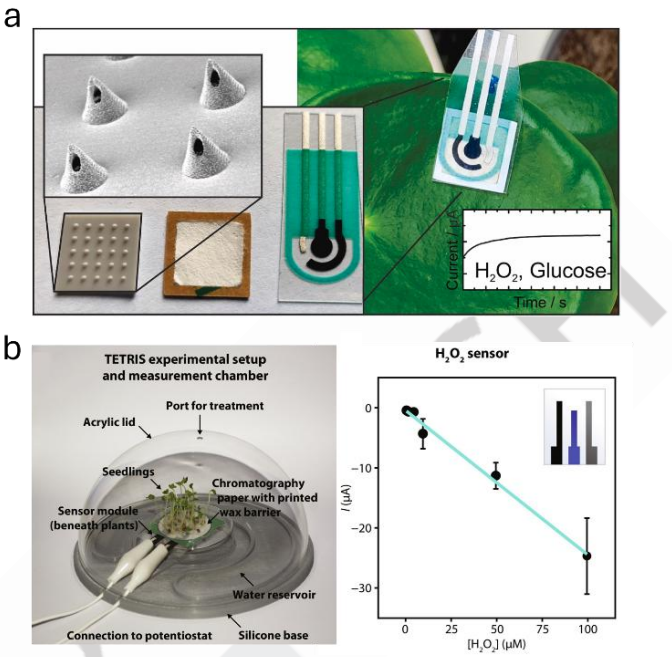

Figure 6: Sensors and setup for detection of reactive oxygen species H_2O_2 in plants.
(a) 3D printed hollow microneedle sensor for profiling of H_2O_2 and glucose. [113] Reproduced with permission from ref [113] Copyright 2024 Elsevier. (b) Setup for whole plant root measurement, with Prussian-blue mediated carbon as working electrode for H_2O_2 detection. [116] Adapted with permission by CC-BY 4.0 license.

Anti-interference membranes are often employed in the detection of small molecules. However, such membranes result in complex fabrication methods and a slower response rate. Kim et al. developed a nitric oxide sensor without the need for additional membranes. [119] The amperometric sensor incorporates the use of Pt nanostructures electrodeposited onto an Au substrate. The selectivity for nitric oxide (NO) detection was enhanced by incorporating sharp-pointed Pt nanostructures with hydrophobic properties, similar to NO. [119] However, this electrode was only used to detect NO gas in phosphate-buffered saline (PBS) solutions and has not been applied for measurements on plants. Further optimization is needed to enable effective monitoring within the plant microclimate.

A spray-coated metallic SWCNT with Ag nanoparticles, with rGO as the sensing material, was presented by Li et al. as a wearable sensor on plants for the detection of nitrogen dioxide (NO_2). [120] Ag nanoparticles were added to improve the performance of the gas sensor by increasing the catalytic activity. The sensing mechanism involves the charge transfer between NO_2 molecules and the rGO layer. The absorption of the NO_2 molecules onto the rGO layer leads to an increase in electrical conductivity due to the higher hole density. The sensor obtains a detection range of 6 to 20 ppm and has a LOD of 0.2 ppm. However, the electrode requires a high-humidity environment for accurate detection of NO_2.

Ammonia, a common reactive nitrogen species from agriculture, can result in toxicity of plants at elevated levels. Additionally, excessive emission of ammonia causes detrimental effects on human health and the ecosystem. Accurate and continuous

monitoring of ammonia levels in agricultural fields is therefore important in ensuring that the ammonia levels are within safe limits. Flexible sensors based on hybrid nanomaterial, polyaniline (PANI) and $Ti_3C_2T_x$ MXene have demonstrated ammonia sensing capabilities over 30 days across a wide humidity range of 20-80% RH and a temperature range of 10-40 °C. [121] The sensor leverages the Schottky junctions at the PANI/$Ti_3C_2T_x$ interface and enhances protonation of hydrochloric acid-doped PANI to improve the gas absorption and detection performance. However, the ageing of the electrode was seen over time in air conditions, and the stability of the electrode towards changing humidity and temperature remains unknown.

3.7. Pathogens

Pathogens cause infectious plant diseases that lead to reduced crop yields, negatively impacting the agricultural economy. A study from the Food and Agricultural Organization found that up to 40% of the agricultural loss was due to pathogens and pests. Some common pathogenic microorganisms include viruses, bacteria and fungi. To prevent widespread diseases in fields, early detection and identification of pathogens are needed to allow effective intervention. Traditional pathogen-detecting techniques include culture-based techniques, [122] which involve isolating and growing suspected pathogens for identification, and molecular techniques, which involve polymerase chain reaction (PCR) or DNA microarrays. [123] These techniques are time-consuming and not cost-effective.

Currently, the most common quantification of pathogens is via the immunoassay method, which is a destructive method that requires plants to be crushed and suspended in a buffer solution before testing can be conducted. [124-126] These immunosensors generally require virus-/bacteria-specific antibodies for detection. However, such antibodies can be expensive and time-consuming to produce. The stability and reusability of antibodies in the long run is also a concern. Emerging non-destructive technologies such as SERS are now being explored for the fast detection of pathogen infection.

To enable non-invasive detection on plants, Kissell et al. developed a hydrogel-based SERS sensor for the detection of tobacco mosaic virus (Figure 7a). [127] The SERS sensor was embedded within the hydrogel matrix, which facilitates the uptake of genetic targets through simple contact with the leaves. The biosensor responds to the presence of the pathogen by exhibiting changes in the SERS signal intensity. In this work, the sensor was able to detect the infection 2 days post-inoculation. This brings about the potential for non-invasive deployable pathogen sensors for plants. However, significant improvements are needed to enhance the long-term stability of the sensor. Additionally, efforts are required to reduce the current detection time of one hour.

3.8. Metabolites and enzymes

Primary metabolites are directly involved in the growth and development of plants. Key primary metabolites involve carbohydrates and amino acids. Common carbohydrate metabolites that are studied include glucose and sucrose, which are involved in energy transport and regulation within plants. On the other hand, amino acid metabolites are protein building blocks which help in stress signaling. Monitoring of primary metabolites is important in understanding the plant's health and metabolic status in its growth cycle. Primary metabolites are also sensitive to any change in their environment and can be used for early detection of stress before any visual observation. In addition, some enzymes have been discovered to reflect the stress condition of plants. Therefore, various non-destructive approaches have been developed to monitor the dynamics of plant metabolites and enzymes (Table 4).

Glucose, being one of the most essential carbohydrates, is directly involved in many critical plant growth processes. Chen et al. developed a microneedle sensor for monitoring glucose levels in plants. [128] The sensing material used was a platinum wire deposited with Au nanoparticles and crosslinked with glucose oxidase. The microneedles were 3D printed with a tip diameter of 300 µm. The sensor was able to achieve a LOD of 33.3 µM. The sensor has also demonstrated the ability to monitor salt stress on plants with real-time monitoring over 12 hours. Next, Perdomo et al. achieve a lower LOD for glucose monitoring at 9.4 µM by integrating a non-invasive enzymatic sensor with reverse iontophoresis fluid extraction. [129] The sensor was able to monitor glucose changes under light and temperature stress.

Apart from glucose, sucrose, and fructose are also carbohydrate metabolites present in plants. Sucrose is responsible for the transport of sugars in the phloem, while fructose is commonly found in fruits and contributes to stress tolerance. Diacci et al. fabricated an implanted enzymatic OECT for *in vivo* real-time monitoring of glucose and sucrose at the xylem (Figure 7b). [130] The diurnal fluctuation of sucrose in aspen was also revealed with this sensor. However, as implantation results in local wound response, the electrode can only be used for monitoring for up to 48 days. Next, Liu et al. demonstrated an enzyme-free electrode for in-situ and in-vivo detection of glucose and fructose via boronic acid-diol recognition. [131] Boronic acids allow selective recognition of glucose and fructose by the formation of cyclic esters. The electrode was modified with a nanocomposite of carboxylated graphene oxide, copper-based MOFs, poly 3-aminophenyl boronic acid (PAPBA) and Nafion for sensing. The use of an artificial neural network (ANN) also allows accurate analysis of the sensor output, achieving detection of glucose in tomatoes.

Proline is a pyrrolidine amino acid and plays a vital role in plant functions. Research has shown that proline helps to maintain cell membrane integrity and protects plants under stress conditions. It is found that proline levels can increase by more than ten times under stress conditions. Hence, Yan et al. developed a molecularly imprinted electrochemical sensor to monitor proline levels. [132] SPE modified with Au nanoparticles were employed. Thionine was used as an internal reference signal, and polypyrrole was the functional monomer for detection. The sensor exhibited a wide detection range from 10^{-16} to 0.01 M with a low LOD of 9.18 aM. Glycine betaine, an amino acid-derived metabolite, plays a critical role in plants during abiotic stress conditions in maintaining cellular osmotic balance and protein levels. Ai et al., from the same research team, further advanced the molecularly imprinted sensor for the detection of glycine betaine. [133] Polydopamine was chosen to fabricate the MIPs.

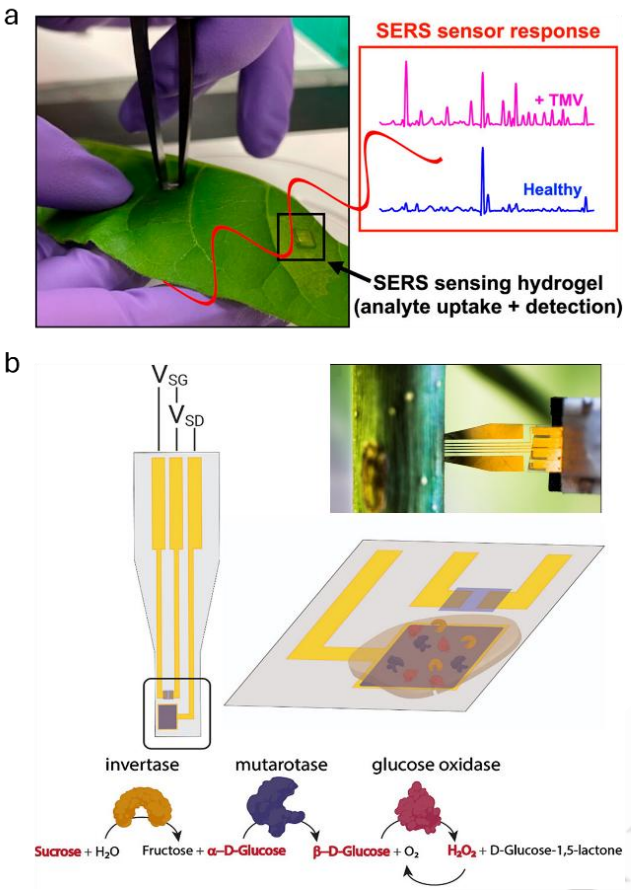

Figure 7: Sensors for detection of pathogens and metabolites in plants. **(a)** Hydrogel-based SERS sensors with the ability to uptake analyte for detection of tobacco mosaic virus. [127] Reproduced with permission from ref [127] Copyright 2024 American Chemical Society. (**b**) Implanted OECT sensor at xylem for monitoring sucrose, glucose and fructose. [130] Reproduced with permission from ref [130] Copyright 2025 Elsevier.

Unlike primary metabolites, secondary metabolites are not directly involved in the primary processes of plant development. [134] Instead, they are commonly found in stress defense interactions or signaling. Khairi et al. demonstrated the monitoring of stigmasterol, a secondary metabolite for G. boninense-infected oil palm, with a beta-cyclodextrin sensor. [135] The sensor was functionalized with rGO and Au nanoparticles. By anchoring the sensor with a redox probe methylene blue, stigmasterol was detected by DPV characterization. Another type of secondary metabolite is vitamins in fruits which are produced only in specific conditions. Liu et al. developed a graphene-based sensor for in-situ detection of melatonin and pyridoxin in fruits. [136] Copper(II) oxide and poly(L-lysine) are the sensing components for melatonin and pyridoxin, respectively. The sensor achieves a LOD of 12 nM for melatonin and 2.3 µM for pyridoxin. Next, a wearable sensor for in-situ and in-vivo detection of quercetin, a flavonoid found in plants, was presented by Wei et al. [137] Au nanoparticles and 2-dimensional black phosphorus nanosheets were fabricated on LIG electrodes to improve stability and sensitivity. The use of a PDMS substrate for the sensor also allows accommodation for stretching and bending of the sensor.

Additionally, an electrochemical sensor was developed for monitoring β-glucuronidase (GUS) enzyme activity in tobacco plants. [138] GUS cleaves β-glucuronic acids to form a detectable blue-colored product. The substrate employed a conjugate of β-glucuronide with another moiety P of either phenolphthalein or p-nitrophenol. During stress response, the substrate diffuses into the plant cell for reaction with the GUS enzyme present and a three-electrode chip was used to detect the enzyme product via oxidation reaction. The electrode showed that the GUS enzyme activity can be used to detect heat stress of plants within 12-26 hours of heat shock, and the LOD of GUS enzyme was 0.1 mM.

Table 4: Detailed performance of sensors for metabolites and enzymes within plants.

Detected metabolite/enzyme	Sensing material	Detection method	Detection range and limit	Plant/sample	Ref
Glucose	Microneedle, Pt wire with Au nanoparticle deposited and crosslinked with glucose oxidase.	CV	100 µM – 100 mM LOD: 33.3 µM	Tomato plant, Aloe vera plant	[128]
	Glucose oxidase, agarose and PVA hydrogel with iontophoretic electrode	Chrono-amperometric	20–80 µM LOD: 9.4 µM LOQ: 28.5 µM	Sweet pepper plant (*Capsicum annuum L.*), Gerbera plant (*Gerbera Jamesonii*), Romaine lettuce plant (*Lactuca sativa L.*)	[129]
Glucose and sucrose	PEN substrate, Ti/Au electrode (source, drain, gate), PEDOT:PSS (channel), with glucose oxidase	CV	100 µM – 1 mM	Hybrid Aspen Tree	[130]
Glucose and fructose	Nafion/PAPBA/GO-COOH-Cu-MOFs/SPE	DPV	1 nM – 1 M LOD: 0.085 nM (glucose), 0.065 nM (fructose)	Tomato fruits, tomato juice	[131]
Proline	MIP/pThi/Au nanoparticles/SPE MIP: Polypyrrole	DPV	10^{-16}–0.01 M LOD: 9.18 aM	Cucumber plants	[132]
Glycine betaine	MIP-COOH-MWCNTs/pThi/Au nanoparticles/SPE MIP: Polydopamine	DPV	1 fmol/L – 10 mmol/L LOD: 0.707 fmol/L	Cucumber plants	[133]
Stigmasterol	β -cyclodextrin functionalized with rGO, Au nanoparticle, redox probe methylene blue	DPV	2–30 µM LOD: 1.5 µM	Oil palm	[135]
Melatonin and pyridoxin	Graphene with CuO and poly(L-lysine) respectively	DPV, amperometric	0.016−1110 µM (Melatonin), 3−2076 µM (Pyridoxin) LOD: 12 nM (Melatonin), 2.3 µM (Pyridoxin)	Orange fruit	[136]
Quercetin	Au nanoparticle/2D black phosphorus/LIG/PDMS	DPV	1–100 µM LOD: 0.65 µM	Strawberry plant	[137]
β-glucuronidase (GUS)	Au-based three-electrode microchip with substrate of p-nitrophenyl-β-glucuronide or phenolphthalein-β-glucuronide	Chrono-amperometric	0.1-1 mM	Transgenic tobacco plant (N.tabacum BY2)	[138]

PVA: poly(vinyl alcohol); PEN: polyethylene naphthalate; PEDOT:PSS: Poly(3,4-ethylenedioxythiophene):poly(styrene sulfonate); PAPBA: poly 3-aminophenylboronic acid; GO-COOH: carboxylated graphene oxide; MOF: metal-organic framework; MIP: molecularly imprinted polymer; COOH-MWCNT: carboxylated multi-walled carbon nanotube; rGO: reduced graphene oxide; SPE: screen-printed electrode; pThi: polythionine; LIG: laser-induced graphene; PDMS: polydimethylsiloxane; CV; cyclic voltammetry; DPV: differential pulse voltammetry; LOD: limit of detection, LOQ: limit of quantification.

3.9. Ions

The ion concentration in the sap provides information on the nutritional status of plants. Changes in ion concentration can reflect the stress conditions of plants and affect the growth of the plants. Ion concentrations are also critical in maintaining the osmoregulation of plants. Furthermore, ions can act as signaling elements during stress response. The monitoring of ion concentration remains mainly invasive to achieve a high sensitivity (Table 5).

With that, Janni et al. developed an invasive OECT sensor inserted at the stem for monitoring ion concentration in the sap. [139] The channel comprises a textile fiber functionalized with PEDOT:PSS for monitoring the changes in ions such as Na^+, K^+, Ca^{2+} and Mg^{2+}. The sensor displayed continuous monitoring for 23 days and successfully detected drought stress within 30 hours of water deprivation. Caselli et al. further explored wireless OECT sensors for monitoring cations. [140] The sensor was also integrated with narrow-band Internet of Things radio interfaces and a web-based server for wireless monitoring. Although the OECT sensors have presented a strong ability to real-time monitor the ion concentrations in plant sap, the OECT sensors were meant to detect total ion concentrations and are unable to achieve discrimination between ions.

In addition, Ibrahim et al. also developed an invasive enzymatic sensor for monitoring nitrate levels in sap. [141] The sensor involves a unique photosensitive epoxy bioresin, with cobalt-based artificial enzyme (Vitamin B12) incorporated into graphene oxide composite. The photosensitive bioresin enables the fabrication of the pyrolytic carbon-based artificial enzyme network through laser writing. The sensor detects nitrate ions by reducing NO_3^- to NO_2^- with the enzyme enhancing the redox reaction through the oxidation of cobalt (Figure 8a). The sensor achieves a detection range from 0.2 to 10 ppm with a year-long shelf life. Furthermore, the sensor was able to discriminate 5 ppm of nitrate from 500 ppm of interference ions such as Ca^{2+}, Na^+, K^+, Cl^- and PO_4^{3-}.

Next, a low-cost solid-state microneedle was presented by Fan et al. for the detection of sodium ions. [142] The stainless steel microneedle was fabricated with a graphene coating followed by electro-polymerization to form a PEDOT:PSS layer. A sodium ion-selective membrane was then applied via dip-coating. The sensor has a response time of 6.8 s with a LOD of 1.94×10^{-6} M. Monitoring of sodium concentration over 3 hours of salt stimulation was demonstrated by the sensor. Wang et al. developed a microneedle sensor for monitoring of potassium and sodium ions (Figure 8b). [143] Stainless steel microneedles were employed and were dip-coated with carbon for the working electrode and silver/silver chloride for the reference electrode. The working electrodes were then functionalized with MWCNT and an ion-selective membrane for detection. The microneedles showed a short response time of <5 s. However, daily replacement or calibration of the electrodes was recommended to reduce signal drift for long-term monitoring. Overall, the use of microneedles and ion-selective membranes has shown the ability to monitor ion concentration in plants, but longer *in vivo* studies should be explored for long-term continuous monitoring.

Apart from invasive methods, Lu et al. developed a wearable guttation sensor for monitoring plant health conditions. [144] Guttation contains plant-derived chemicals (carbohydrates, proteins, enzymes), microbial chemicals (toxins, mycotoxins) and inorganic chemicals (salts, ions, nutrients). The sensor employs a colorimetric microfluidic chip and allows concurrent monitoring of different parameters, including acephate, lead, hardness, nitrate, nitrite and pH levels. However, significant improvements are needed in the sensors' sensitivity and ability to be reused.

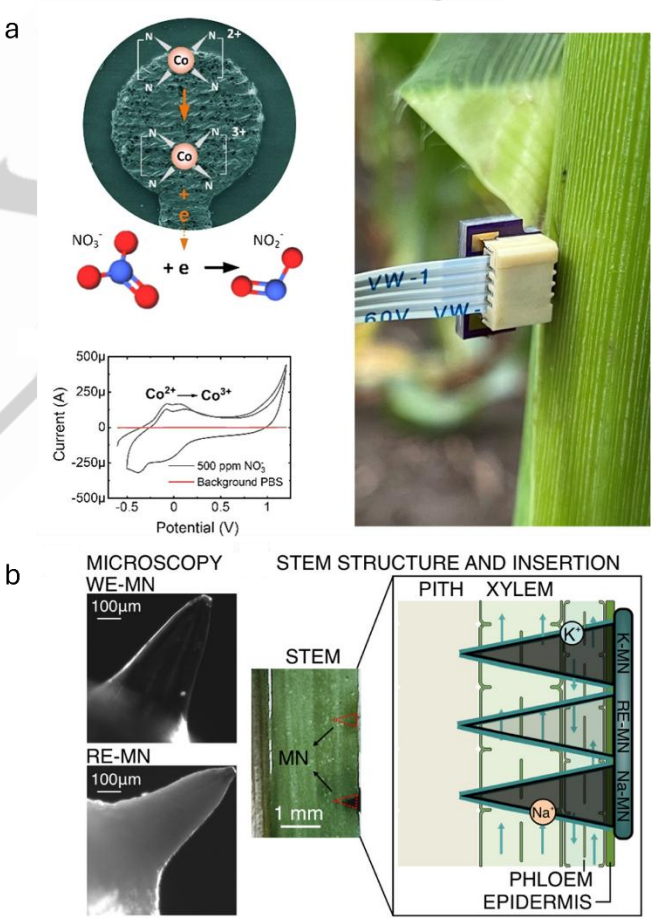

Figure 8: Devices for measurement of plant ionic concentrations.
(a) Invasive enzymatic sensor for detection of nitrate levels, with change in oxidation state of cobalt to reduce NO_3^- to NO_2^-. [141] Adapted with permission from ref [141] Copyright 2022 American Chemical Society. (b) Microneedle sensor for concurrent monitoring of potassium and sodium levels. [143] WE-MN: working electrode microneedle; RE-MN: reference electrode microneedle. Adapted with permission by CC-BY 4.0 license.

Table 5: Detailed performance of sensors for ion detection within plants.

Detected ions	Sensing material	Detection method	Detection range and limit	Plant/sample	Ref
Ions (non-selective)	Invasive OECT based on textile fibers functionalized with PEDOT:PSS	Transistor electrical characterization	-	Tomato plant (*cv. Red Setter*)	[139]
Ions (non-selective)	Invasive cotton wires functionalized with PEDOT:PSS	Transistor electrical characterization	Up to 10 mM of sodium	-	[140]
Nitrate	Pyrolytic carbon-based artificial enzyme network	CV	0.2–10 ppm	Maise plant (B73 genotype)	[141]
Sodium	Stainless steel microneedle/graphene with PEDOT:PSS and ion-selective membrane	CV	10^{-2}–10^{-5}M LOD: 1.94×10^{-6} M	Rice seedlings	[142]
Potassium, sodium	Stainless steel microneedle/carbon, functionalized with MWCNT and ion selective membrane	Potentiometric	50–120nM (Potassium), 5–50 mM (Sodium)	Basil plant (*Ocimum basilicum*)	[143]
Nitrate, nitrite	Commercial test strips on Japanese paper	Colorimetric	-	Tomato plant	[144]

OECT: organic electrochemical transistors; PEDOT:PSS: Poly(3,4-ethylenedioxythiophene):poly(styrene sulfonate); MWCNT: multi-walled carbon nanotube; CV: cyclic voltammetry; LOD: limit of detection.

4. Summary and Outlook

Chemical sensors have demonstrated promising potential in monitoring plant health indicators such as the presence of environmental toxins, VOCs, phytohormones and metabolites. Substantial progress has been made in enhancing the sensitivity and selectivity of the sensors. The use of chemical sensors for in-situ monitoring of plants has proven effective in the early detection of stress conditions, potentially allowing early intervention for stress mitigation (Figure 9). There is a noticeable shift towards wearable and flexible sensors, which offer real-time monitoring capabilities and are better suited for in-field applications. Meanwhile, the progress and potential of nanosensors, i.e., functionalized nanomaterials delivered into plants for chemical visualization, are noticeable. The recently explored techniques for non-destructive chemical sensing are mainly electrochemical methods and optical methods. However, each type of sensor presents specific challenges that must be addressed to enhance the sensor's performance. For enzyme-mediated electrochemical sensors, the stability of the enzymes tends to be affected by the environmental conditions. In contrast, non-enzyme-mediated electrochemical and chemiresistive sensors have better stability but are intrinsically inferior in specificity and selectivity. Special techniques are making progress in addressing this problem, including surface functionalization with MIPs, antibodies, and aptamers. [145-146] Additionally, different testing protocols (DPV, SWV, etc.) help to minimize peak overlaps, while pattern analysis of sensor arrays helps to improve the overall selectivity. Anti-interference membranes are often used to block unwanted analytes, but sensor sensitivity will be negatively affected. Therefore, careful balancing of sensor sensitivity and selectivity is essential to achieve an accurate detection of the target analyte. Colorimetric sensors offer on-site detection capabilities, providing farmers with a direct visual cue for alerts. However, their reusability is often limited, posing challenges for continuous monitoring, and their selectivity is generally poor. Fluorescent methods are increasingly utilizing nanomaterials with fluorescence quenching properties for effective biomarker monitoring. As these nanomaterials are directly injected into plants, further research is required to evaluate their long-term toxicity. Additionally, the impact of these nanosensors on plant stress responses remains unexplored. Due to the low detection limit and quick detection, SERS has been found to be a promising technique for non-destructive testing on plants. Fluorescent testing and SERS have also provided the mapping capability for the study of spatiotemporal monitoring. Wearable SERS sensors are also of high interest due to their high specificity for the simultaneous detection of multiple biomarkers. However, the sensitivity of SERS sensors is highly influenced by environmental factors, which may lead to unreliable results. Furthermore, there is a need to develop a more portable Raman spectrometer to achieve in-field deployment. Besides these technique-specific bottlenecks, current chemical sensors for plants share common challenges in long-term monitoring, low-cost deployment, and multi-modal sensing, which are some of the key barriers that currently limit the widespread field adoption of plant sensors.

4.1 Real-time and long-term monitoring

Real-time detection provides prompt notice of the presence of stress and the ability to mitigate the negative impacts within a short period of time. However, many of the techniques introduced here, though being non-destructive, are not designed for continuous monitoring in the field, such as colorimetric sensors and SERS. System-level design is needed to address this issue, which encompasses sensing mechanism, sensor form factor, detection equipment deployment, data transmission, etc.

Long-term continuous measurement is essential for the detection of stress in field applications. This requires addressing the environmental and physical challenges the sensors may face. Current sensor testing is often conducted in controlled environments, unlike the dynamic conditions in the field, where factors such as temperature and humidity fluctuate. It is crucial that the sensors can adapt to these changes and maintain accurate detection. In addition, long-term deployment on plants necessitates consideration of mechanical disturbances, such as wind and rain. A secure, conformal attachment of sensors is needed to avoid interference from mechanical noise. Furthermore, the sensors should have a minimal impact on the daily physiological processes of the plants, such as gas exchange. The sensors must be of high transmittance to prevent interference with light absorption. They should also accommodate plant growth in the sensor application area without hindering the plant's development. To address these problems, substantial innovations in materials are needed.

4.2 Production and deployment

Although plant-wearable sensors have garnered significant research interest, scaling them for large-scale field deployment remains challenging. Addressing this requires overcoming several practical issues. First, developing low-cost manufacturing

methods is essential to enable large-scale production and deployment. Sensor production should focus on machine fabrication to ensure high reproducibility and scalability. Importantly, the feasibility of applying sensors to individual plants should be evaluated, and alternative solutions such as sparse sampling and machine-aided sensor application should be explored. Sensor applications should be simplified for easy adoption by farmers. Furthermore, the environmental impact of large-scale deployment of plant sensors must be addressed by exploring sustainable solutions [147]. For instance, biocompatible and biodegradable cellulose materials [60] were explored as a more sustainable material solution for plant sensors. Additionally, low-powered devices should be developed as a priority. Effective powering solutions, such as self-powering through energy harvesting from the environment and plants, are urgently needed. [148] Furthermore, wireless signal transmission coupled with a cloud database should be incorporated into the system design while keeping the power consumption low. This can be challenging in remote agricultural areas, and energy-efficient data transmission technologies are essential.

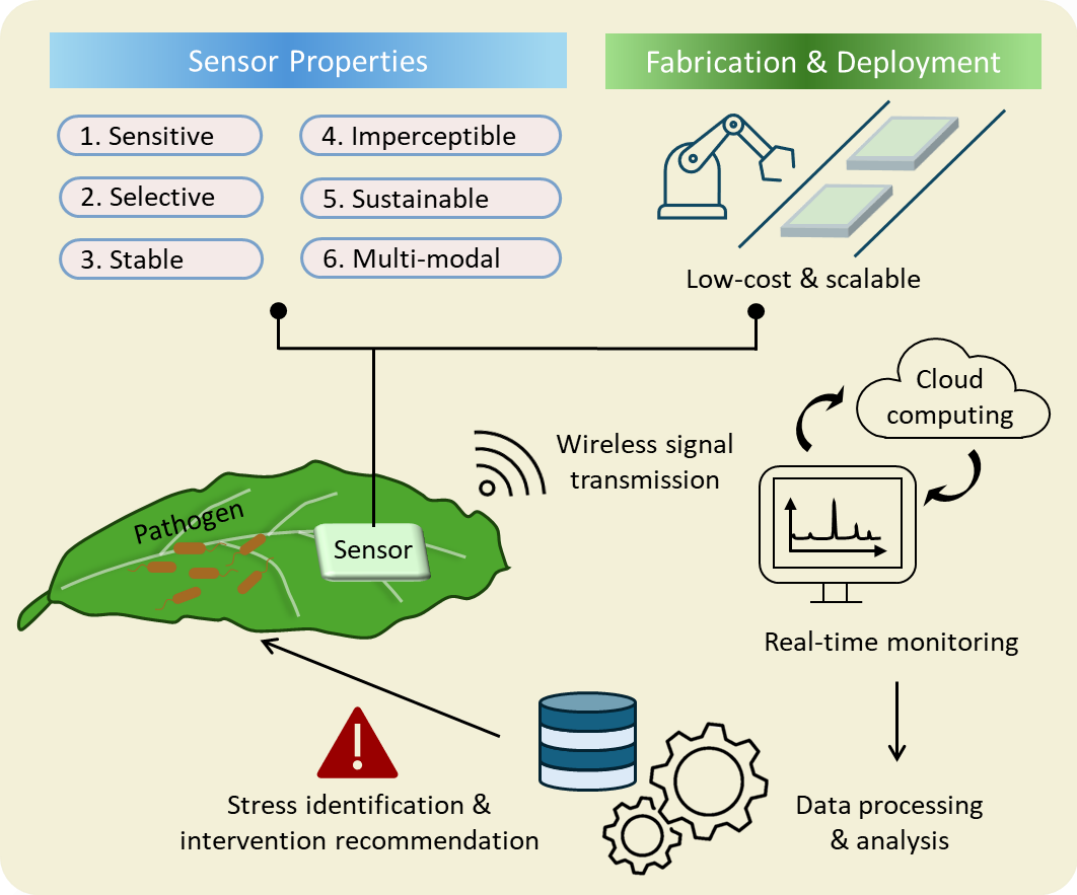

Figure 9: Outlook of chemical sensors for in-field plant detection.

4.3 Multi-modal detection and data analysis

Current sensor development mainly focuses on single biomarker detection, which is often insufficient for stress identification towards effective intervention. Future work should incorporate multi-biomarker detection for a more precise detection of stress. The selectivity and sensitivity of the sensor for multiple biomarkers should be optimized through electrode functionalization and testing protocols to prevent interference among results. For multi-modal sensors, efforts should be made towards miniaturization of both the sensor and data acquisition system to improve portability, reduce interference to plants, and increase the spatial resolution of detected signals. However, reducing electrode size during this process can significantly diminish the output current, affecting the performance of electrochemical sensors. Additionally, current studies on stress detection with biomarkers typically focus on single-stress conditions, limiting their applicability to complex, multi-stress scenarios in real-world agricultural environments.

Furthermore, accurate identification and differentiation of stress conditions require advanced data analysis. To enable more precise identification and classification of stress factors, constructing a comprehensive database which incorporates data from diverse plant species under various environmental conditions is essential for reference and trend analysis. With the availability of the database, artificial intelligence can be leveraged to analyze complex and large datasets for efficient and effective decision-making (Figure 9).

In conclusion, non-destructive plant chemical sensors are still in its infancy stage of development. Although current progress shows great promise in achieving unprecedented sensing capabilities compared to conventional methods, the real-world deployment remains elusive. Many bottlenecks exist, awaiting innovations from researchers across diverse disciplines. Since

agriculture is in general a low profit-margin industry, the cost and benefit of sensor application is especially crucial. While other industries may be explored, non-destructive plant chemical sensing remains a powerful and potentially revolutionary tool for fundamental study of plant physiology and pathology.

Acknowledgements

The authors thank the funding support by Agency for Science, Technology and Research (A*STAR) under the Manufacturing, Trade and Connectivity (MTC) Programmatic funding scheme (M23L8b0049) and Career Development Fund (C233312018).

Keywords: chemical sensors • plant biomarkers • wearable sensors • nanosensors • biosensors

References

[1] A. Steensland, M. Zeigler, Global Harvest Initiative, **2018**
[2] E. C. Oerke, *J. Agric. Sci.* **2006**, *144*, 31-43.
[3] N. Suzuki, R. M. Rivero, V. Shulaev, E. Blumwald, R. Mittler, *New Phytol.* **2014**, *203*, 32-43.
[4] I. Secretariat, *Scientific review of the impact of climate change on plant pests – A global challenge to prevent and mitigate plant pest risks in agriculture, forestry and ecosystems.*, FAO on behalf of the IPPC Secretariat, **2021**.
[5] K. Pawlak, M. Kołodziejczak, *Sustain.* **2020**, *12*, 5488.
[6] M. C. Hunter, R. G. Smith, M. E. Schipanski, L. W. Atwood, D. A. Mortensen, *BioScience* **2017**, *67*, 386-391.
[7] M. K. Lal, R. K. Tiwari, M. A. Altaf, A. Kumar, R. Kumar, *Front. Plant Sci.* **2023**, *14*, 1212982.
[8] S. Peck, R. Mittler, *J. Exp. Bot.* **2020**, *71*, 1649-1651.
[9] J. H. Li, L. F. Fan, D. J. Zhao, Q. Zhou, J. P. Yao, Z. Y. Wang, L. Huang, *J. Plant Physiol.* **2021**, *261*, 153418.
[10] A. Christmann, E. Grill, J. Huang, *Curr. Opin. Plant Biol.* **2013**, *16*, 293-300.
[11] P. Coatsworth, L. Gonzalez-Macia, A. S. P. Collins, T. Bozkurt, F. Güder, *Nat. Rev. Chem.* **2023**, *7*, 7-25.
[12] B. I. Musah, *Environ. Monit. Assess.* **2024**, *197*, 12.
[13] H. Gautam, S. Singh, H. Prashad, A. Kumar, A. Choudhary, H. Kaur, O. P. Narayan, S. K. Lal, S. Mehta, in *Plants and Their Interaction to Environmental Pollution* (Ed.: A. Husen), Elsevier, **2023**, pp. 231-252.
[14] M. F. Ahmad, F. A. Ahmad, A. A. Alsayegh, M. Zeyaullah, A. M. AlShahrani, K. Muzammil, A. A. Saati, S. Wahab, E. Y. Elbendary, N. Kambal, M. H. Abdelrahman, S. Hussain, *Heliyon* **2024**, *10*, e29128.
[15] Y. Posudin, in *Methods of Measuring Environmental Parameters*, **2014**, pp. 229-243.
[16] L. Makhlouf, K. El Fakhouri, S. A. Kemal, A. Aasfar, I. Meftah Kadmiri, M. El Bouhssini, *Front. hortic.* **2024**, *3*.
[17] D. Cao, M. He, *Front. Plant Sci.* **2023**, *14*.
[18] D. Khanal, A. Dhital, A. Neupane, K. Paudel, M. Shrestha, N. Upadhyaya, R. Bhandari, P. Pandey, *J. King Saud Univ. Sci.* **2023**, *35*, 102671.
[19] S. Zhou, J. Zhou, Y. Pan, Q. Wu, J. Ping, *Trends Plant Sci.* **2023**, *29*, 219-231.
[20] S. Lee, J. Kim, D. Kim, H. Park, S. Myoung, J. Han, C. Park, Y. Kim, C. Choi, G. Lee, *Adv. Sustain. Syst.* **2024**, *8*, 2300634.
[21] B. Wang, H. Lu, S. Jiang, B. Gao, *Anal. Bioanal. Chem.* **2024**, *416*, 55–69.
[22] A. Bharti, U. Jain, N. Chauhan, *Plant Nano Biol.* **2024**, *9*, 100079.
[23] M. C. Ang, T. T. S. Lew, *Front. Plant Sci.* **2022**, *13*, 884454.
[24] K. He, C. Wang, Y. He, J. Su, X. Chen, *Chem. Rev.* **2023**, *123*, 13796-13865.
[25] Y. Luo, M. R. Abidian, J.-H. Ahn, D. Akinwande, A. M. Andrews, M. Antonietti, Z. Bao, M. Berggren, C. A. Berkey, C. J. Bettinger, J. Chen, P. Chen, W. Cheng, X. Cheng, S.-J. Choi, A. Chortos, C. Dagdeviren, R. H. Dauskardt, C.-a. Di, M. D. Dickey, X. Duan, A. Facchetti, Z. Fan, Y. Fang, J. Feng, X. Feng, H. Gao, W. Gao, X. Gong, C. F. Guo, X. Guo, M. C. Hartel, Z. He, J. S. Ho, Y. Hu, Q. Huang, Y. Huang, F. Huo, M. M. Hussain, A. Javey, U. Jeong, C. Jiang, X. Jiang, J. Kang, D. Karnaushenko, A. Khademhosseini, D.-H. Kim, I.-D. Kim, D. Kireev, L. Kong, C. Lee, N.-E. Lee, P. S. Lee, T.-W. Lee, F. Li, J. Li, C. Liang, C. T. Lim, Y. Lin, D. J. Lipomi, J. Liu, K. Liu, N. Liu, R. Liu, Y. Liu, Y. Liu, Z. Liu, Z. Liu, X. J. Loh, N. Lu, Z. Lv, S. Magdassi, G. G. Malliaras, N. Matsuhisa, A. Nathan, S. Niu, J. Pan, C. Pang, Q. Pei, H. Peng, D. Qi, H. Ren, J. A. Rogers, A. Rowe, O. G. Schmidt, T. Sekitani, D.-G. Seo, G. Shen, X. Sheng, Q. Shi, T. Someya, Y. Song, E. Stavrinidou, M. Su, X. Sun, K. Takei, X.-M. Tao, B. C. K. Tee, A. V.-Y. Thean, T. Q. Trung, et al., *ACS Nano* **2023**, *17*, 5211-5295.
[26] G. Lee, Q. Wei, Y. Zhu, *Adv. Funct. Mater.* **2021**, *31*, 2106475.
[27] W. Xu, L. Chen, X. Hu, L. Zhang, D. Huang, J. Li, R. Xiong, C. Huang, M. Zhu, *Adv. Funct. Mater.* **2024**, *34*, 2410544.
[28] C. Zhang, J. Kong, D. Wu, Z. Guan, B. Ding, F. Chen, *Plant Phenomics* **2023**, *5*, 0051.
[29] X. H. Li, M. Z. Li, J. Y. Li, Y. Y. Gao, C. R. Liu, G. F. Hao, *Plant Biotechnol. J.* **2024**, *22*, 1516-1535.
[30] S. Banerji, H. Hõrak, J. Torop, T.-P. Huynh, *Adv. Sens. Res.* **2024**, *3*, 2300023.
[31] K. Muthumalai, N. Gokila, Y. Haldorai, R. T. Rajendra Kumar, *Adv. Sens. Res.* **2023**, *3*, 2300107.
[32] C. Lv, C. Hu, J. Luo, S. Liu, Y. Qiao, Z. Zhang, J. Song, Y. Shi, J. Cai, A. Watanabe, *Nanomaterials* **2019**, *9*, 422.
[33] S. A. John, A. Chattree, P. W. Ramteke, P. Shanthy, T. A. Nguyen, S. Rajendran, in *Nanosensors for Smart Agriculture* (Eds.: A. Denizli, T. A. Nguyen, S. Rajendran, G. Yasin, A. K. Nadda), Elsevier, **2022**, pp. 449-461.
[34] Z. Guo, J. J. Richardson, B. Kong, K. Liang, *Sci. Adv.* **2020**, *6*, eaaz0330.
[35] P. Sicard, *Curr. Opin. Environ. Sci. Health* **2021**, *19*, 100226.
[36] N. E. Grulke, R. L. Heath, *Plant Biol.* **2020**, *22*, 12-37.
[37] G. Lorenzini, C. Saitanis, in *Abiotic Stresses in Plants* (Eds.: L. S. di Toppi, B. Pawlik-Skowrońska), Springer Netherlands, Dordrecht, **2003**, pp. 205-229.
[38] P. Vollenweider, M. Ottiger, M. S. Günthardt-Goerg, *Environ. Pollut.* **2003**, *124*, 101-118.
[39] N. Gosselin, V. Sagan, M. Maimaitiyiming, J. Fishman, K. Belina, A. Podleski, M. Maimaitijiang, A. Bashir, J. Balakrishna, A. Dixon, *Remote Sens.* **2020**, *12*, 93.
[40] K. Borowiak, R. Rucińska-Sobkowiak, K. Rymer, E. A. Gwóźdź, J. Zbierska, *Pol. J. Ecol.* **2009**, *57*, 3-14.
[41] J. J. Kim, R. Fan, L. K. Allison, T. L. Andrew, *Sci. Adv.* **2020**, *6*, eabc3296.
[42] P. C. Nagajyoti, K. D. Lee, T. V. M. Sreekanth, *Environ. Chem. Lett.* **2010**, *8*, 199-216.
[43] N. Singh, Sourabh, P. Kumar, Preeti, S. Mehta, in *Plants and Their Interaction to Environmental Pollution* (Ed.: A. Husen), Elsevier, **2023**, pp. 253-264.
[44] S. Seker, O. Surucu, A. Economou, J. Wang, *Talanta* **2025**, *287*, 127654.
[45] S. Manavalan, G. Cho, H. S. Kim, S. M. Jung, *J. Hazard. Mater.* **2025**, *491*, 137981.
[46] J. Liang, M. Y. B. Zulkifli, S. Choy, Y. Li, M. Gao, B. Kong, J. Yun, K. Liang, *Environ. Sci. Technol.* **2020**, *54*, 11356-11364.
[47] T. T. S. Lew, M. Park, J. Cui, M. S. Strano, *Adv. Mater.* **2021**, *33*, 2005683.
[48] M. W. Aktar, D. Sengupta, A. Chowdhury, *Interdiscip. Toxicol.* **2009**, *2*, 1-12.
[49] R. Kaur, D. Choudhary, S. Bali, S. S. Bandral, V. Singh, M. A. Ahmad, N. Rani, T. G. Singh, B. Chandrasekaran, *Sci. Total Environ.* **2024**, *915*, 170113.
[50] G. Yu, W. Wu, Q. Zhao, X. Wei, Q. Lu, *Biosens. Bioelectron.* **2015**, *68*, 288-294.
[51] M. Wei, J. Wang, *Sens. Actuators B Chem.* **2015**, *211*, 290-296.

[52] S. Wu, F. Huang, X. Lan, X. Wang, J. Wang, C. Meng, *Sens. Actuators B Chem.* **2013**, *177*, 724-729.
[53] H.-F. Cui, W.-W. Wu, M.-M. Li, X. Song, Y. Lv, T.-T. Zhang, *Biosens. Bioelectron.* **2018**, *99*, 223-229.
[54] S. Nagabooshanam, S. Roy, S. Deshmukh, S. Wadhwa, I. Sulania, A. Mathur, S. Krishnamurthy, L. M. Bharadwaj, S. S. Roy, *ACS Omega* **2020**, *5*, 31765-31773.
[55] L. Zhang, Y. Sun, Z. Zhang, Y. Shen, Y. Li, T. Ma, Q. Zhang, Y. Ying, Y. Fu, *Biosens. Bioelectron.* **2022**, *216*, 114659.
[56] F. Zhao, J. He, X. Li, Y. Bai, Y. Ying, J. Ping, *Biosens. Bioelectron.* **2020**, *170*, 112636.
[57] C. Zhou, J. Feng, Y. Tian, Y. Wu, Q. He, G. Li, J. Liu, *Environ. Sci. Adv.* **2023**, *2*, 933-956.
[58] M. I. Hossain, M. A. Hasnat, *Heliyon* **2023**, *9*, e19299.
[59] R. T. Paschoalin, N. O. Gomes, G. F. Almeida, S. Bilatto, C. S. Farinas, S. A. S. Machado, L. H. C. Mattoso, O. N. Oliveira, Jr., P. A. Raymundo-Pereira, *Biosens. Bioelectron.* **2022**, *199*, 113875.
[60] S. C. Teixeira, N. O. Gomes, M. L. Calegaro, S. A. S. Machado, T. V. de Oliveira, N. de Fátima Ferreira Soares, P. A. Raymundo-Pereira, *Biomater. Adv.* **2023**, *155*, 213676.
[61] X. Yan, Y. Ma, Y. Lu, C. Su, X. Liu, H. Li, G. Lu, P. Sun, *Adv. Mater.* **2024**, e2311144.
[62] X. Yi, Z. Yuan, X. Yu, L. Zheng, C. Wang, *ACS Appl. Mater. Interfaces* **2023**, *15*, 4873-4882.
[63] A. Mohan, L. Chandran, K. G. Gopchandran, *ACS Appl. Opt. Mater.* **2024**, *2*, 574-584.
[64] F. Farshchi, A. Saadati, H. Kholafazad-Kordasht, F. Seidi, M. Hasanzadeh, *J. Mol. Recognit.* **2021**, *34*, e2927.
[65] P. A. Raymundo-Pereira, N. O. Gomes, F. M. Shimizu, S. A. S. Machado, O. N. Oliveira, *Chem. Eng. J.* **2021**, *408*, 127279.
[66] D. Egamberdieva, S. J. Wirth, A. A. Alqarawi, E. F. Abd_Allah, A. Hashem, *Front. Microbiol.* **2017**, *8*, 02104.
[67] J. Ali, M. Mukarram, J. Ojo, N. Dawam, R. Riyazuddin, H. A. Ghramh, K. A. Khan, R. Chen, D. Kurjak, A. Bayram, *Physiol. Plant.* **2024**, *176*, e14307.
[68] V. G. Checker, H. R. Kushwaha, P. Kumari, S. Yadav, in *Molecular Aspects of Plant-Pathogen Interaction* (Eds.: A. Singh, I. K. Singh), Springer Singapore, Singapore, **2018**, pp. 159-184.
[69] S. Vanneste, J. Friml, *Cell* **2009**, *136*, 1005-1016.
[70] W. D. Teale, I. A. Paponov, K. Palme, *Nat. Rev. Mol. Cell Biol.* **2006**, *7*, 847-859.
[71] A. Ali, K. Kant, N. Kaur, S. Gupta, P. Jindal, S. S. Gill, M. Naeem, *S. Afr. J. Bot.* **2024**, *169*, 314-335.
[72] L. Sun, S. Xu, Y. Tang, Y. Zhou, M. Wang, Y. Tian, G. Li, X. Zhu, N. Bao, L. Sun, *Anal. Bioanal. Chem.* **2022**, *414*, 7721-7730.
[73] L. Tang, D. Li, W. Liu, Y. Tang, R. Zhang, Y. Tian, R. Tan, X. Yang, L. Sun, *Anal. Chim. Acta* **2024**, *1316*, 342875.
[74] A. H. Bukhamsin, S. S. Shetty, E. Fakeih, M. S. Martinez, C. Lerma, M. Mundummal, J. Y. Wang, J. Kosel, S. Al-Babili, I. Blilou, K. N. Salama, *Sci. Adv.* **2025**, *11*, eads8733.
[75] X. Zhang, Y. Zhou, J. Wang, X. Huang, H. S. El-Mesery, Y. Shi, Y. Zou, Z. Li, Y. Li, J. Shi, X. Zou, *Food Chem.* **2025**, *467*, 142342.
[76] M. C. Ang, N. Dhar, D. T. Khong, T. T. S. Lew, M. Park, S. Sarangapani, J. Cui, A. Dehadrai, G. P. Singh, M. B. Chan-Park, R. Sarojam, M. Strano, *ACS Sens.* **2021**, *6*, 3032-3046.
[77] A. Singh, A. Roychoudhury, *Plant Cell Rep.* **2023**, *42*, 961-974.
[78] Z. Wang, L. Xue, M. Li, C. Li, P. Li, H. Li, *Mater. Sci. Eng. C* **2021**, *127*, 112237.
[79] M. Li, P. Zhou, X. Wang, Y. Wen, L. Xu, J. Hu, Z. Huang, M. Li, *Comp. Electron. Agr.* **2021**, *191*, 106502.
[80] S. A. Perdomo, D. P. Valencia, G. E. Velez, A. Jaramillo-Botero, *Biosens. Bioelectron.* **2024**, *255*, 116261.
[81] S. Khazaee Nejad, H. Ma, A. Al-Shami, A. Soleimani, M. A. Mohamed, P. Dankwah, H. J. Lee, M. P. S. Mousavi, *Sens. Diagn.* **2024**, *3*, 400-411.
[82] A. Bukhamsin, A. Ait Lahcen, J. O. Filho, S. Shetty, I. Blilou, J. Kosel, K. N. Salama, *Biosens. Bioelectron.* **2022**, *214*, 114515.
[83] X. Yu, W. Zhang, Y. Zhang, X. Zhang, D. Lang, X. Zhang, *Funct. Plant Biol.* **2019**, *46*, 197-212.
[84] C. Li, P. Wang, N. W. Menzies, E. Lombi, P. M. Kopittke, *J. Plant Nutri. Soil Sci.* **2018**, *181*, 409-418.
[85] A. Larrieu, A. Champion, J. Legrand, J. Lavenus, D. Mast, G. Brunoud, J. Oh, S. Guyomarc'h, M. Pizot, E. E. Farmer, C. Turnbull, T. Vernoux, M. J. Bennett, L. Laplaze, *Nat. Commun.* **2015**, *6*, 6043.
[86] P. Shu, Y. Li, J. Sheng, L. Shen, *J. Agric. Food Chem.* **2024**, *72*, 4552-4563.
[87] L. T. d. C. Bungala, C. Park, J. E. L. Dique, R. Sathasivam, S. Y. Shin, S. U. Park, *Insects* **2024**, *15*, 404.
[88] F. Nazir, P. Peter, R. Gupta, S. Kumari, K. Nawaz, M. I. R. Khan, *Physiol. Plant.* **2024**, *176*, e14151.
[89] N. I. Hossain, S. Tabassum, *Sci. Rep.* **2023**, *13*, 9848.
[90] N. I. Hossain, T. Noushin, S. Tabassum, *IEEE Sens. J.* **2023**, *3327547*, 1.
[91] S.-Y. Jeong, Y. K. Moon, T.-H. Kim, S.-W. Park, K. B. Kim, Y. C. Kang, J.-H. Lee, *Adv. Sci.* **2020**, *7*, 1903093.
[92] X. Li, R. Sun, J. Pan, Z. Shi, J. Lv, Z. An, Y. He, Q. Chen, R. P. S. Han, F. Zhang, Y. Lu, H. Liang, Q. Liu, *Small* **2023**, *19*, 2207889.
[93] A. Brosset, J. D. Blande, *J. Exp. Bot.* **2021**, *73*, 511-528.
[94] L. A. Burkle, J. B. Runyon, *Funct. Ecol.* **2019**, *33*, 2116-2129.
[95] J. Midzi, D. W. Jeffery, U. Baumann, S. Rogiers, S. D. Tyerman, V. Pagay, *Plants* **2022**, *11*, 2566.
[96] Y. Liu, H. Zhang, S. Umashankar, X. Liang, H. W. Lee, S. Swarup, C. N. Ong, *Metabolites* **2018**, *8*, 94.
[97] G. Vivaldo, E. Masi, C. Taiti, G. Caldarelli, S. Mancuso, *Sci. Rep.* **2017**, *7*, 11050.
[98] Y. L. Dorokhov, E. V. Sheshukova, T. V. Komarova, *Front. Plant Sci.* **2018**, *9*, 01623.
[99] P. Harley, J. Greenberg, Ü. Niinemets, A. Guenther, *Biogeosciences* **2007**, *4*, 1083-1099.
[100] H. Ibrahim, S. Moru, P. Schnable, L. Dong, *ACS Sens.* **2022**, *7*, 2293-2302.
[101] M. Heil, J. C. Silva Bueno, *Proc. Natl. Acad. Sci. U. S. A.* **2007**, *104*, 5467-5472.
[102] A. Ficke, B. Asalf, H. R. Norli, *Front. Microbiol.* **2022**, *12*, 803352.
[103] C. Zheng, Q. a. Zhou, J. Wang, D. Du, *Sens. Actuators B Chem.* **2023**, *381*, 133408.
[104] Y. Fang, Y. Umasankar, R. P. Ramasamy, *Analyst* **2014**, *139*, 3804-3810.
[105] Z. Li, Y. Liu, O. Hossain, R. Paul, S. Yao, S. Wu, J. B. Ristaino, Y. Zhu, Q. Wei, *Matter* **2021**, *4*, 2553-2570.
[106] G. Lee, O. Hossain, S. Jamalzadegan, Y. Liu, H. Wang, A. C. Saville, T. Shymanovich, R. Paul, D. Rotenberg, A. E. Whitfield, J. B. Ristaino, Y. Zhu, Q. Wei, *Sci. Adv.* **2023**, *9*, eade2232.
[107] X. Wang, H. Qi, Y. Shao, M. Zhao, H. Chen, Y. Chen, Y. Ying, Y. Wang, *Adv. Sci.* **2024**, *11*, 2400207.
[108] Y. S. Choi, W. K. Son, H. Kwak, J. Park, S. Choi, D. Sim, M. G. Kim, H. Kimm, H. Son, D. H. Jeong, S.-Y. Kwak, *Adv. Sci.* **2025**, *12*, 2412732.
[109] Y. Fichman, G. Miller, R. Mittler, *Mol. Plant* **2019**, *12*, 1203-1210.
[110] S. J. Swanson, W.-G. Choi, A. Chanoca, S. Gilroy, *Annu. Rev. Plant Biol.* **2011**, *62*, 273-297.
[111] T. T. S. Lew, V. B. Koman, K. S. Silmore, J. S. Seo, P. Gordiichuk, S.-Y. Kwak, M. Park, M. C.-Y. Ang, D. T. Khong, M. A. Lee, M. B. Chan-Park, N.-H. Chua, M. S. Strano, *Nat. Plants* **2020**, *6*, 404-415.
[112] Y. Yao, X. Liu, Y. Shao, Y. Ying, J. Ping, *Biosens. Bioelectron.* **2020**, *166*, 112463.
[113] M. Parrilla, A. Sena-Torralba, A. Steijlen, S. Morais, A. Maquieira, K. De Wael, *Biosens. Bioelectron.* **2024**, *251*, 116131.
[114] C. Zhang, X. Wu, S. Yao, Y. Shao, C. Zhang, S. Zhou, J. Ping, Y. Ying, *Engineering* **2024**, *11*, 021.

[115] H. Wen, L. Kong, X. Zhu, Y. Miao, X. Sheng, X. Chen, Y. Liu, P. Chen, *The Innovation*, 100800.
[116] P. Coatsworth, Y. Cotur, A. Naik, T. Asfour, A. S.-P. Collins, S. Olenik, Z. Zhou, L. Gonzalez-Macia, D.-Y. Chao, T. Bozkurt, F. Güder, *Sci. Adv.* **2024**, *10*, eadj6315.
[117] M. Mandal, M. Sarkar, A. Khan, M. Biswas, A. Masi, R. Rakwal, G. K. Agrawal, A. Srivastava, A. Sarkar, *Adv. Redox Res.* **2022**, *5*, 100039.
[118] M. Khan, S. Ali, T. N. I. Al Azzawi, S. Saqib, F. Ullah, A. Ayaz, W. Zaman, *Antioxidants* **2023**, *12*, 268.
[119] S. Kim, Y. Ha, S.-j. Kim, C. Lee, Y. Lee, *Analyst* **2019**, *144*, 258-264.
[120] W. Li, C. Teng, Y. Sun, L. Cai, J.-L. Xu, M. Sun, X. Li, X. Yang, L. Xiang, D. Xie, T. Ren, *ACS Appl. Mater. Interfaces* **2018**, *10*, 34485-34493.
[121] X. Li, J. Xu, Y. Jiang, Z. He, B. Liu, H. Xie, H. Li, Z. Li, Y. Wang, H. Tai, *Sens. Actuators B Chem.* **2020**, *316*, 128144.
[122] M. Ray, A. Ray, S. Dash, A. Mishra, K. G. Achary, S. Nayak, S. Singh, *Biosens. Bioelectron.* **2017**, *87*, 708-723.
[123] M. Venbrux, S. Crauwels, H. Rediers, *Front. Plant Sci.* **2023**, *14*, 1120968.
[124] T. A. Freitas, C. A. Proença, T. A. Baldo, E. M. Materón, A. Wong, R. F. Magnani, R. C. Faria, *Talanta* **2019**, *205*, 120110.
[125] H. Haji-Hashemi, P. Norouzi, M. R. Safarnejad, B. Larijani, M. M. Habibi, H. Raeisi, M. R. Ganjali, *J. Electroanal. Chem.* **2018**, *820*, 111-117.
[126] M. Berto, E. Vecchi, L. Baiamonte, C. Condò, M. Sensi, M. Di Lauro, M. Sola, A. De Stradis, F. Biscarini, A. Minafra, C. A. Bortolotti, *Sens. Actuators B Chem.* **2019**, *281*, 150-156.
[127] L. N. Kissell, H. Liu, M. Sheokand, D. Vang, P. Kachroo, P. Strobbia, *ACS Sens.* **2024**, *9*, 514-523.
[128] H. Chen, S. Zhou, J. Chen, J. Zhou, K. Fan, Y. Pan, J. Ping, *Biosens. Bioelectron.* **2024**, *248*, 115964.
[129] S. A. Perdomo, E. De la Paz, R. Del Caño, S. Seker, T. Saha, J. Wang, A. Jaramillo-Botero, *Biosens. Bioelectron.* **2023**, *231*, 115300.
[130] C. Diacci, T. Abedi, J. W. Lee, E. O. Gabrielsson, M. Berggren, D. T. Simon, T. Niittylä, E. Stavrinidou, *iScience* **2021**, *24*, 101966.
[131] K. Liu, T. Xu, A. Li, C. Zhao, *Comp. Electron. Agr.* **2024**, *218*, 108714.
[132] L. Yan, B. Luo, C. Wang, H. Dong, X. Wang, P. Hou, K. Liu, A. Li, *ChemElectroChem* **2024**, *11*, e202300538.
[133] G. Ai, Y. Zhou, H. Zhang, Q. Wei, B. Luo, Y. Xie, C. Wang, X. Xue, A. Li, *Food Chem.* **2024**, *435*, 137554.
[134] L. Yang, K.-S. Wen, X. Ruan, Y.-X. Zhao, F. Wei, Q. Wang, *Molecules* **2018**, *23*, 762.
[135] N. A. S. Khairi, N. A. Yusof, J. Abdullah, I. A. Seman, N. Ithnin, A. S. F. A, *IEEE Sens. J.* **2024**, *24*, 9341-9352.
[136] Y. Liu, M. Li, H. Li, G. Wang, Y. Long, A. Li, B. Yang, *ACS Sustain. Chem. Eng.* **2019**, *7*, 19537-19545.
[137] H. Wei, K. Liu, H. Zhang, P. Hou, D. Pan, B. Luo, A. Li, C. Zhao, *Chem. Eng. J.* **2024**, *497*, 154271.
[138] R. Pandey, O. Teig-Sussholz, S. Schuster, A. Avni, Y. Shacham-Diamand, *Biosens. Bioelectron.* **2018**, *117*, 493-500.
[139] M. Janni, N. Coppede, M. Bettelli, N. Briglia, A. Petrozza, S. Summerer, F. Vurro, D. Danzi, F. Cellini, N. Marmiroli, D. Pignone, S. Iannotta, A. Zappettini, *Plant Phenomics* **2019**, *2019*, 6168209.
[140] M. Caselli, E. Graiani, V. Bianchi, F. Vurro, M. Bettelli, G. Tarabella, I. D. Munari, M. Janni, A. Boni, *IEEE Transactions on AgriFood Electronics* **2024**, *2*, 268-275.
[141] H. Ibrahim, S. Yin, S. Moru, Y. Zhu, M. J. Castellano, L. Dong, *ACS Appl. Mater. Interfaces* **2022**, *14*, 25949-25961.
[142] C.-X. Fan, Z. Wang, Z.-H. Wang, A.-W. Wang, Z.-Y. Wang, L. Huang, *Anal. Chim. Acta.* **2025**, *1352*, 343892.
[143] Q. Wang, Á. Molinero-Fernández, J.-R. Acosta-Motos, G. A. Crespo, M. Cuartero, *ACS Sens.* **2024**, *9*, 5214-5223.
[144] Q. Lu, L. Yang, A. Maheshwari, H. Ni, T. Yu, J. Gu, A. Wadhwani, H. Xu, A. Danielescu, L. Yao, in *Extended Abstracts of the CHI Conference on Human Factors in Computing Systems, Vol. 183*, Association for Computing Machinery, Honolulu, HI, USA, **2024**, pp. 1-9.
[145] C. Zhou, J. Feng, Y. Tian, Y. Wu, Q. He, G. Li, J. Liu, *Environ. Sci.: Adv.* **2023**, *2*, 933-956.
[146] M. Majdinasab, M. Daneshi, J. Louis Marty, *Talanta* **2021**, *232*, 122397.
[147] S. C. Teixeira, N. O. Gomes, T. V. d. Oliveira, P. Fortes-Da-Silva, N. d. F. F. Soares, P. A. Raymundo-Pereira, *Biosens. Bioelectron. X* **2023**, *14*, 100371.
[148] S. Wang, Y. Chai, H. Sa, W. Ye, Q. Wang, Y. Zou, X. Luo, L. Xie, X. Liu, *Sci. Adv.* **2024**, *10*, eads1136.

Entry for the Table of Contents

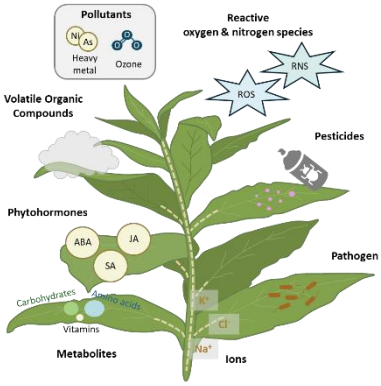

This review presents recent advancements in the use of non-destructive methods for plant chemical sensing. It summarizes the different environmental chemicals and plant biomarkers used for assessing plant health. The paper also discusses various types of sensing devices and techniques, along with emerging use of flexible and wearable devices on plants.